This Research Was Sponsored by
The Space Nuclear Propulsion Office - NASA/AEC
Under Grant NsG - 728

A HYBRID SERVO-POSITIONING SYSTEM FOR A COMPUTER CONTROLLED MANIPULATOR

Report 1-66-41

by

Peter W. Hammond

Dr. H. W. Mergler
Professor of Engineering
Principal Investigator
Grant NsG-728

1966

ABSTRACT

An experimental facility for investigating computer control of a manipulator is described. The design features of part of the computer/machine interface are presented, including circuit details of a digital-to-analog convertor, an R. C. Active filter, and a phase-switching servo-amplifier. The packaging of the various components is displayed. A basic manipulator control program illustrates the general function of the facility.

TABLE OF CONTENTS

LIST OF FIGURES

LIST OF SYMBOLS

a_i, b_i, c_i	discrete variables in a sumation
a	azimuth angle
A	dimensionless constant, such as gain
C_1, C_2, C_3	values of capacitance
D_N	an N-bit binary number
d_i	the i th bit of D_N
DE	an incremental value of E
DELB	a computer program address of DE
e	elevation angle
E_L	the voltage output of a ladder network
E_p	the voltage output of a potentiometer
E.M.F.	electro-motive force in a motor
E	elbow pivot angle from vertical
e_F	level detector trip voltage
F	an optimizing criterion
F_{min}	the best value of F
FMIN	a computer program address of F_{min}
FET	field effect transistor
g_1, g_2, g_3	values of conductance
g	differential gain

I_E	inertia of E
i_o	quiescent current
I	series motor current
M	magnitude of sine wane
N	series motor speed
N_c	critical value of N
R	resistance, as of motor
SCR	silicon controlled rectifier
S	shoulder pivot angle
s	Laplace complex operator
T	torque of series motor
To	quiescent delay
T_1, T_2	controlled delays
T(s), T(w)	voltage transfer ratio
V_{peak}	maximum instantaneous voltage
W	wrist pivot angle
w	angular frequency
X	bridge position variable
x	Cartesian ordinate variable
Y	carriage position variable
y	Cartesian absicca variable
Z	hoist position variable

z	Cartesian height variable
α	potentiometer set angle
σ	maximum value of α
ϕ	SCR firing angle
ϕ_{min}	minimum value of ϕ
θ	shoulder rotation angle

CHAPTER I

INTRODUCTION

Objectives

Considerable interest has been shown recently in improving remote manipulation[1]. One promising possibility is the inclusion of a Process Control Computer in the system. An advantage of this approach is that the computer can organize and even partially assume the control of a multitude of inter-related functions; presenting the operator with a new set of commands that is smaller and simpler but more meaningful. The goals of the manipulation studies at Case are to demonstrate the feasibility of computer-assisted control, and to develop computer programs that augment the manipulator's effectiveness.

Facilities

To permit the investigation of such a system, a test facility has been established. This consists of the following equipment:

1. A Computer Control Corporation DDP-116 process-control computer is available for real-time on-line use.

2. A general Mills Model 100 overhead manipulator has been modified and installed in an adjacent laboratory.

3. An Interface system has been designed and constructed to permit direct control of the manipulator by the computer.

These components are pictured in Figures 1, 2, and 3 respectively.

Capabilities

The Case DDP-116 has a memory capacity of 8,192 16-bit words, with a 1.7 micro-second memory cycle time. Hardware for multiplication, division, and direct memory access is included; and the I/O equipment consists of an ASR-33 teletype, a high-speed paper tape reader and punch, a magnetic tape transport, an IBM-card reader, and a general purpose interface. Software includes DAP and Fortran IV assemblers with subroutines.

The modified Model 100 manipulator consists of an overhead support structure which provides north-south, east-west, and vertical mobility. This structure carries an arm which can be rotated about the vertical axis, and has articulated shoulder, elbow, and wrist joints. The arm is terminated by a hand or a hook that can grasp or twist, giving it a reach of 56 inches. The manipulator can carry 50 pounds in any position,

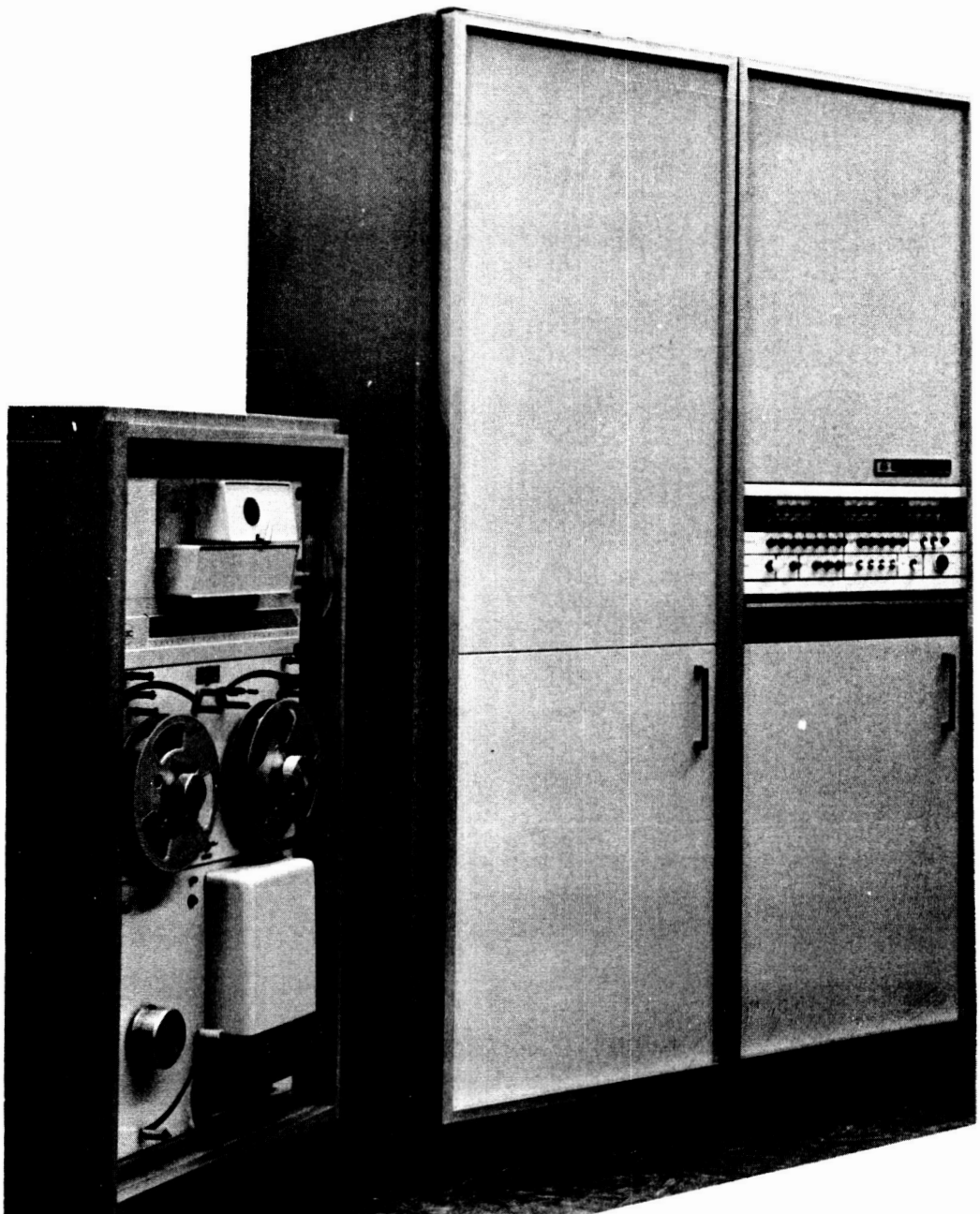

FIGURE 1: THE DDP 116 COMPUTER

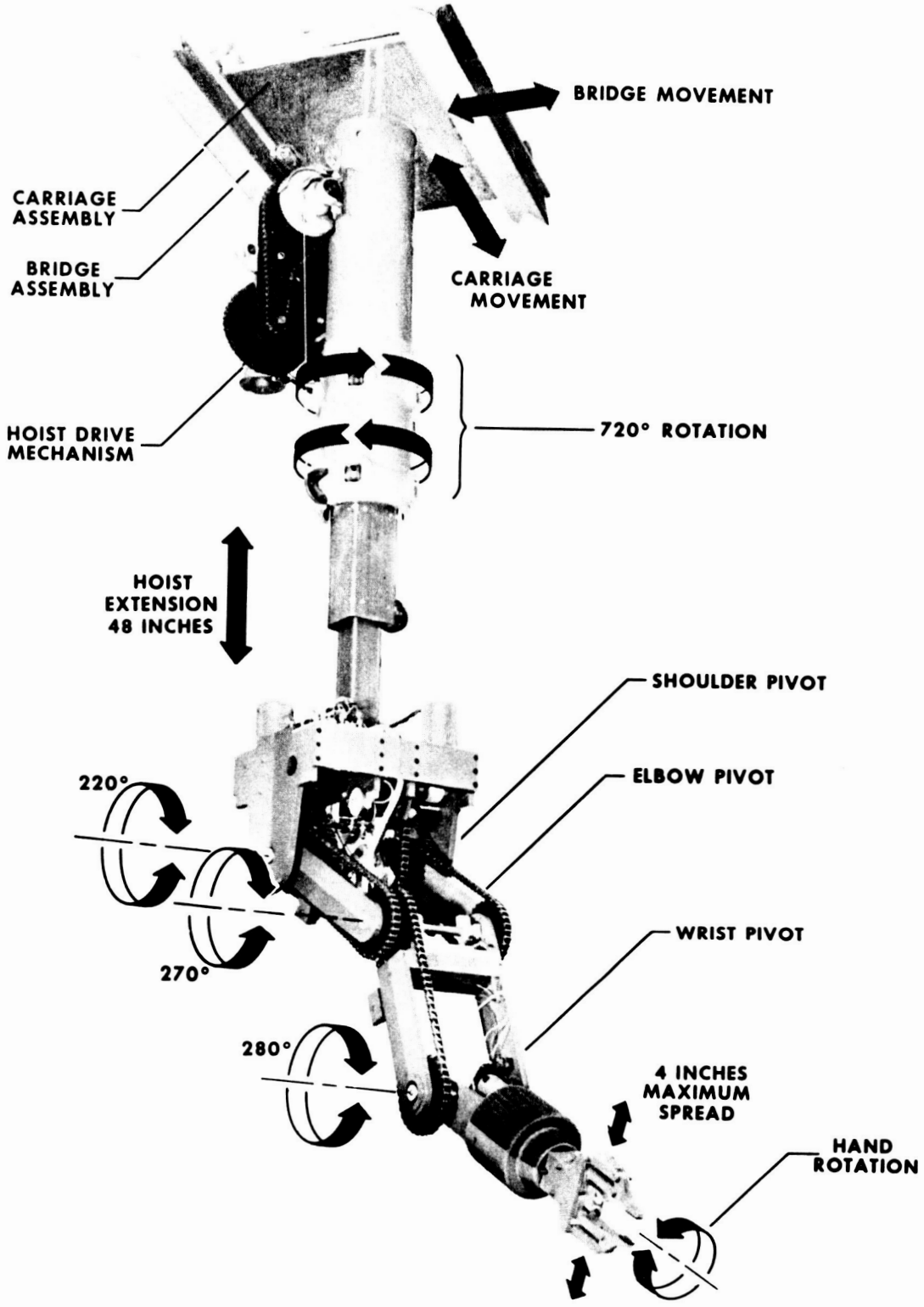

FIGURE 2: THE MODIFIED MODEL 100 MANIPULATOR

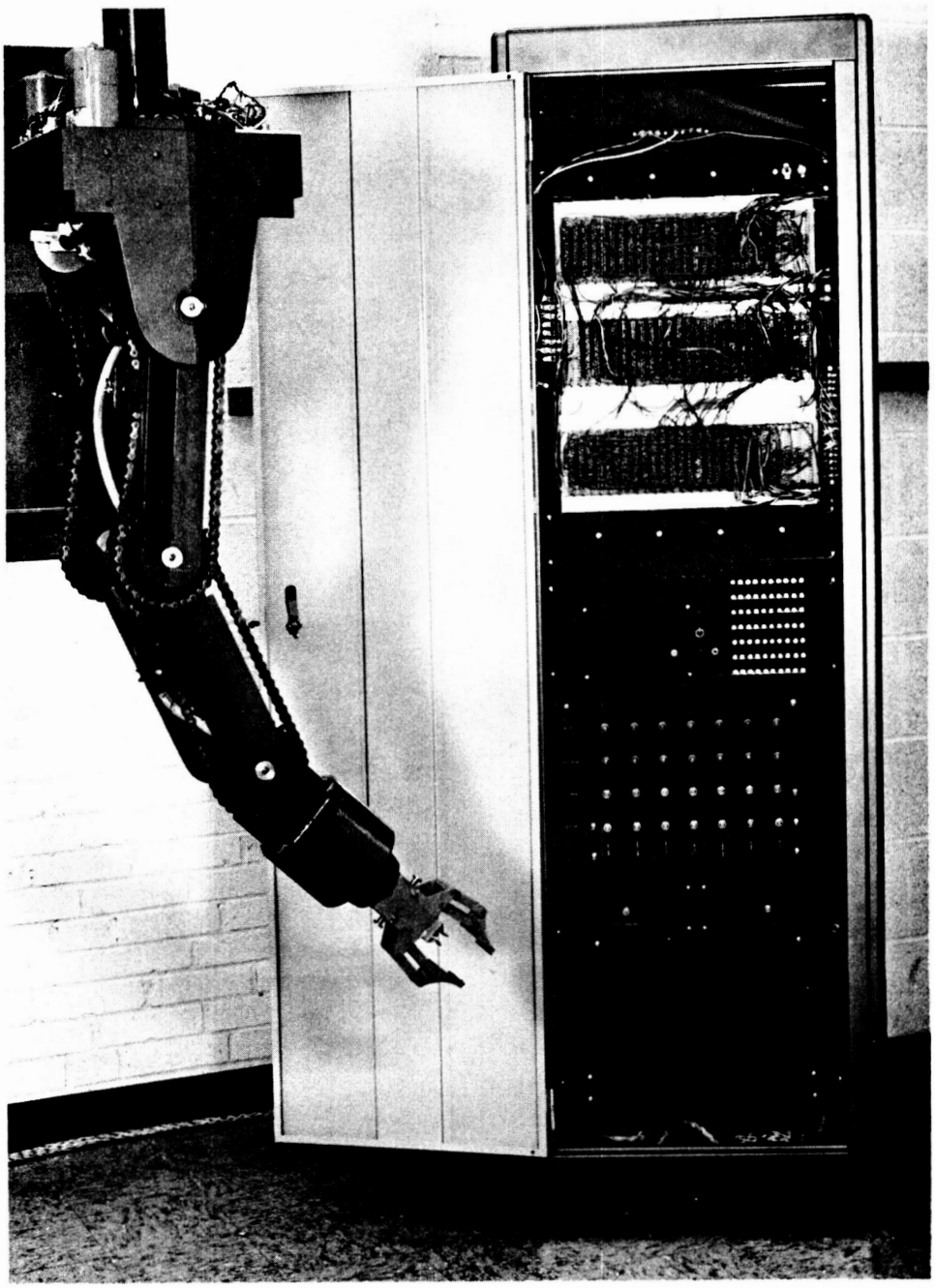

FIGURE 3: THE INTERFACE SYSTEM

and has an average hand speed per controlled axis of 100 inches per minute. The nine driving points with their respective functions and ranges are listed below:

1. The bridge provides north-south travel of 175 inches.

2. The carriage provides east-west travel of 146 inches.

3. The hoist provides vertical travel of 48 inches.

4. The shoulder rotation provides two revolutions of rotation about the vertical axis.

5. The shoulder pivot provides 220 degrees of rotation about a horizontal axis.

6. The elbow pivot provides 270 degrees of rotation about a horizontal axis.

7. The wrist pivot provides 280 degrees of rotation about a horizontal axis.

8. The wrist rotation provides continuous rotation of the hand about its axis.

9. The hand grip may be opened or closed.

System Structure

The control structure of the manipulating facility is diagrammed in Figure 4. The teletype is used to instruct the computer to perform a particular manipulating task. The computer operates on these instructions according to its previously entered program and produces the appropriate manipulator

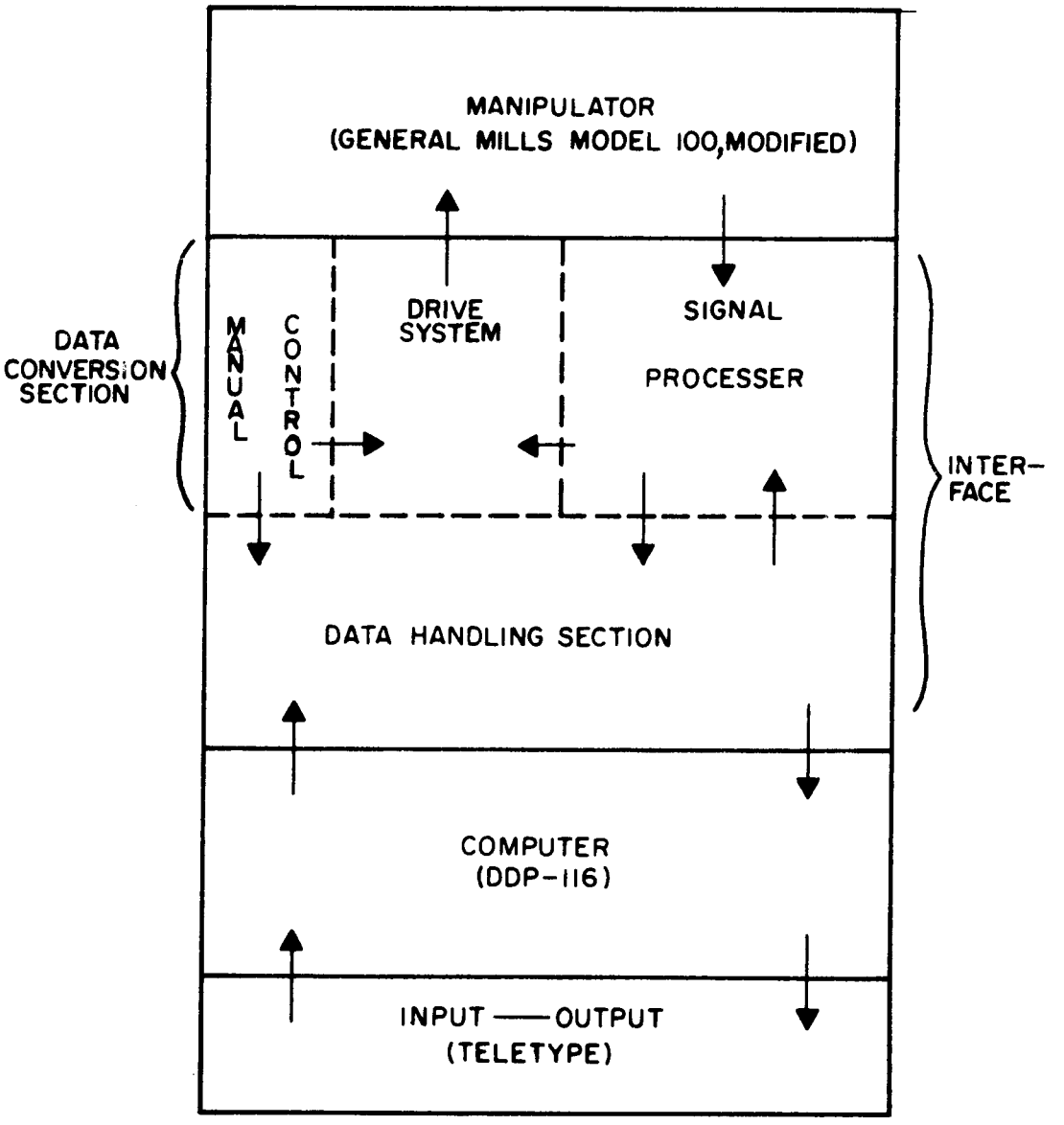

FIGURE 4: CONTROL STRUCTURE

control signals. The Interface consists of two sections. The data handling (digital) section routes the computer commands to assigned storage locations. The data conversion (analog) section converts these commands to a corresponding geometric configuration of the manipulator. This in turn requires a signal processor and drive system. A manual controller can directly control the manipulator. In this mode information flows from the manipulator through the signal processor and data handling system to the computer.

Organization

The detailed descriptions of the manipulator modifications, the data handling and storage portion of the interface, and the computer techniques appear elsewhere[2, 3]. This paper is devoted to the conversion section of the Interface. The organization is as follows:

Chapter II discusses the specifications and requirements on the Interface system, and describes its operating principles. The design philosophy of the data conversion section is outlined.

Chapter III describes in detail the design and implementation of the signal processing equipment.

Chapter IV describes in detail the design and implement-

ation of the prime movers and drive amplifiers.

Chapver V describes the physical layout and packaging of the circuitry.

Appendix A presents a simple manipulator control program.

CHAPTER II

THE DATA CONVERSION SYSTEM

Function

The original plans for the manipulation test facility specify that the computer have control of seven axes of the manipulator. The computer exercises absolute position control over these parameters, with a resolution of one part in 1024. In other words, the computer specifies the desired configuration of the manipulator by giving a vector of seven ten-bit binary numbers. The manipulator may also be controlled manually, in which case the controlled axes assume velocities proportional to the control signals (the deflection of a lever). The remaining driving points, the hand grip and wrist rotate, have two-speed manual control, with simple on-off computer control.

In addition to specifying a desired configuration for the manipulator, the computer must also be able to determine the current configuration. This means a vector of seven ten-bit numbers corresponding to the configuration must be assembled and returned to the computer on request. It is the purpose of the Interface system to execute these control functions.

Requirements

The structure of the interface is as follows: Seven ten-bit storage registers are provided, one for each controlled parameter. Logic circuitry permits the computer to either output to, or input from these registers in a prescribed sequence. The registers drive digital-to-analog convertors to produce a voltage proportional to their numerical content. These voltages become the inputs to separate servo-positioning systems, in which an error voltage is formed by comparison to a feedback transducer on the manipulator and amplified to drive an electric motor. In the manual mode the drive amplifiers are excited by manual controls to move the manipulator. The error voltages, generated as above, drive null detectors which indicate whether the register contents overstate, agree with, or understate the true manipulator position. In the data handling logic, the null detector values can then be arranged into a digital word and transmitted to the computer, which makes successive approximation adjustments to the registers until agreement is obtained. Alternately, the registers can be converted to bi-directional counters, and the null detector outputs used to gate a clock frequency into the forward or backward inputs. This method does not provide as rapid analog-to-digital conversion

as that of successive approximation, but does enable the registers to track the manipulator while it is moving under manual control. The computer can interrogate the registers while tracking is in progress.

Design Formulation

The data conversion (or analog) portion of the interface therefore contains seven similar sub-systems each consisting of:

1. A digital-to-analog convertor
2. A position feedback transducer
3. A voltage comparator
4. An amplifier and prime mover
5. A null detector

The design of such a system involves two basic choices, namely the type of prime mover and drive amplifier, and the method of processing the low-level signals. The first choice was resolved to series-wound universal motors with phase-switched SCR amplifiers because:

1. The speed, torque, and input power of a series motor are related in a manner well suited to driving a manipulator.
2. The manipulator already had four such motors, and the three more required for modification were available with the desired gearheads at low cost.

3. There is no quiescent power dissipation in a series motor, and it is well suited to SCR drive.

The second choice was resolved to d.c. voltage signals because:

1. The SCR drives accept a d.c. input.

2. The cost was minimal, since precision potentiometers can be used as feedback transducers and no demodulation is necessary.

3. It was determined that the desired resolution and noise rejection could be obtained with d.c.

The resulting block diagram of a typical data conversion sub-system is shown in Figure 5. The differential comparator must include some form of noise filtering, as will be demonstrated. In addition to the separate but identical sub-systems, peripheral equipment such as common power supplies and control circuitry are required.

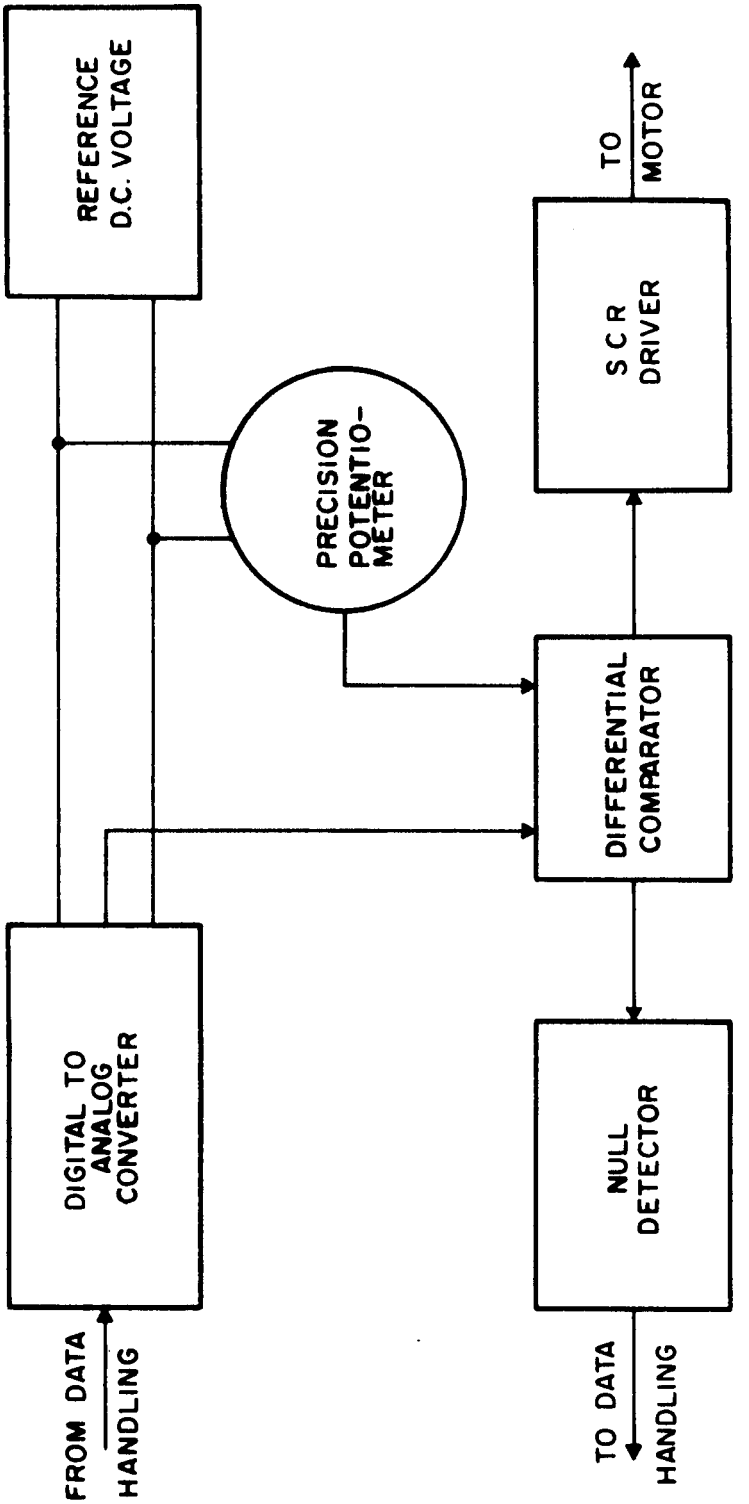

FIGURE 5: DATA CONVERSION SUB-SYSTEM

CHAPTER III

THE SIGNAL PROCESSOR

Requirements

As outlined in Chapter II, the inputs to the positioning systems from the computer are stored in binary form in separate buffer registers. These registers drive digital to analog convertors, whose outputs are compared with the position feedback signal to obtain the error. The error signal has two functions:

1. During automatic (computer controlled) operation of the manipulator, the error is amplified by the servo-amplifier to drive the motor.
2. During manual (operator controlled) operation, the error is used to control the amount and direction of a series of corrections to the register contents.

A precision servo-potentiometer with d.c. voltage feedback is used as the most economical method of obtaining a position feedback signal. The problems associated with this approach are:

1. Forming the error signal with the necessary resolution (one part per thousand). This requires either a very high reference voltage and a comparator which can accept such voltages, or a very low drift, high gain comparator.
2. Removing line-syncronous noise. The servo-amplifier is sensitive to noise at frequencies which are even multiples of the line frequency; and the wires from the potentiometers, being adjacent to the motor power leads, will encounter

such noise.

Design Philosophy

To circumvent the first problem, the feedback potentiometer and the digital-to-analog convertor are connected in a bridge configuration. This has the advantage that it forms the error, or difference signal directly, so that a high reference voltage is possible and no comparator is needed. Further, variations in the reference voltage affect the gain but not the error, so that a precision source is unnecessary. However, it requires the digital-to-analog convertor, the potentiometer, and the reference source to be isolated from ground, so that a separate reference supply for each channel is required. To isolate the digital-to-analog convertor, it is driven with reed relays; which also contributes to the accuracy of conversion.

To eliminate the induced line-syncronous noise, a low-pass filter precedes the input to the servo-amplifier. Since this filter must provide good rejection at 60 cps. without destroying the closed-loop stability, it must be moderately sophisticated. Due to the size and expense of inductors for low frequencies and high impedance levels, the R.C. Active technique of filter realization is adopted. It developed that realistic reference levels required additional gain preceding the servo-amplifier,

and the R. C. Active filter also performs this function.

The control signals to correct the register contents are generated by a null detector which is driven by the filter. A switching relay connects the servo-amplifier to the filter for automatic operation or to an external voltage divider for manual operation. The block diagram of this system is shown in Figure 6.

Digital-to-Analog Convertor Design

The method of digital-to-analog conversion chosen is the voltage-controlled ladder network. This converter circuit is shown in Figure 7. It consists of a sequence of voltage sources in an iterative resistor ladder. The output of this ladder is [4]:

$$E_L = \sum_{i=1}^{N} \frac{e_i}{2^{(i)}} \qquad (1)$$

If the voltage sources can assume only two values, V_{ref} and zero; we have:

$$E_L = \frac{V_{ref}}{2^{(N)}} \sum_{i=1}^{N} d_i \; 2^{(i-1)} \qquad (2=$$

where d_i is either one or zero and indicates the condition of e_i. But the summation in equation (2) is just the value of an N-bit binary number:

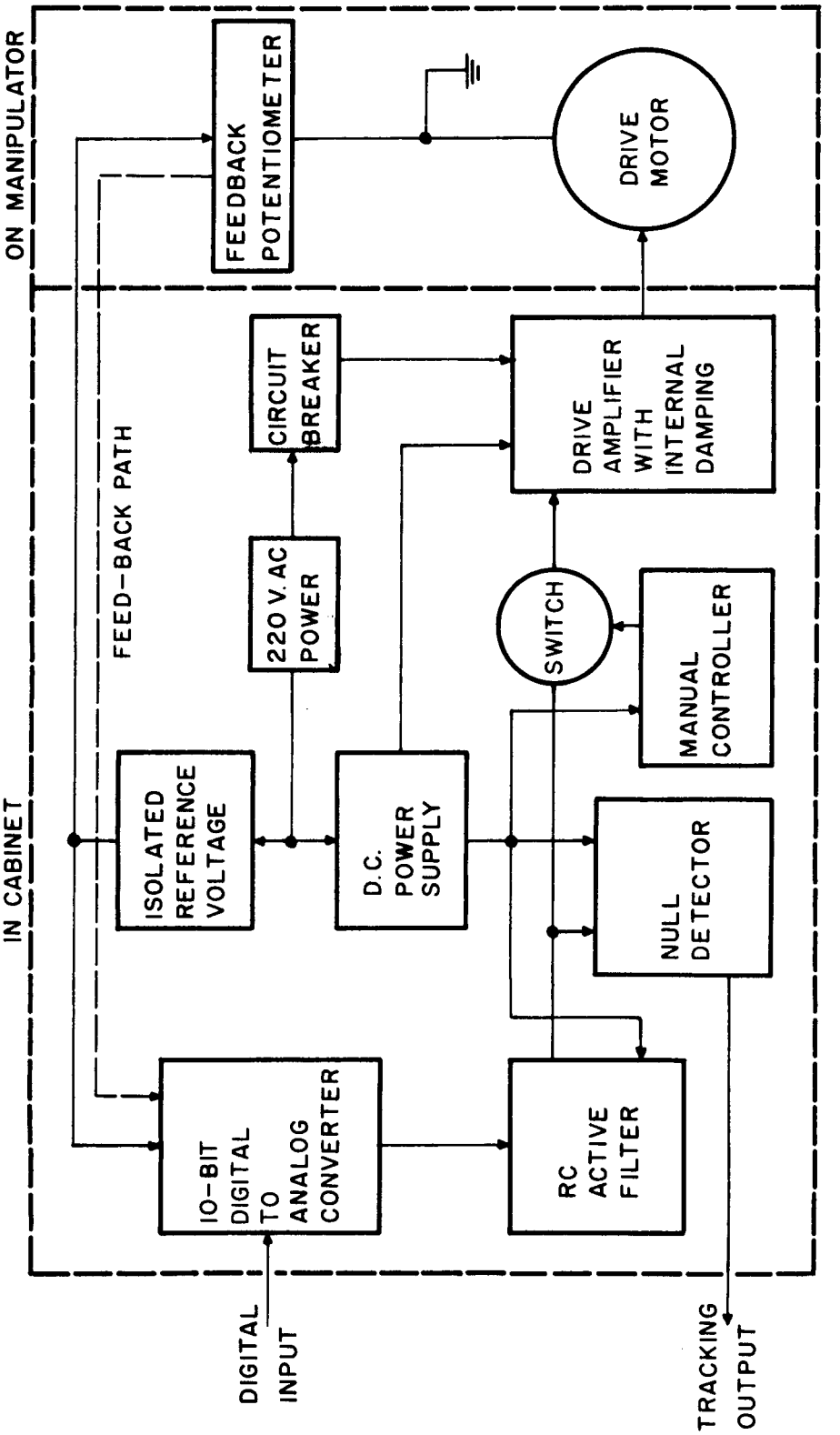

FIGURE 6: BLOCK DIAGRAM OF SUB-SYSTEM

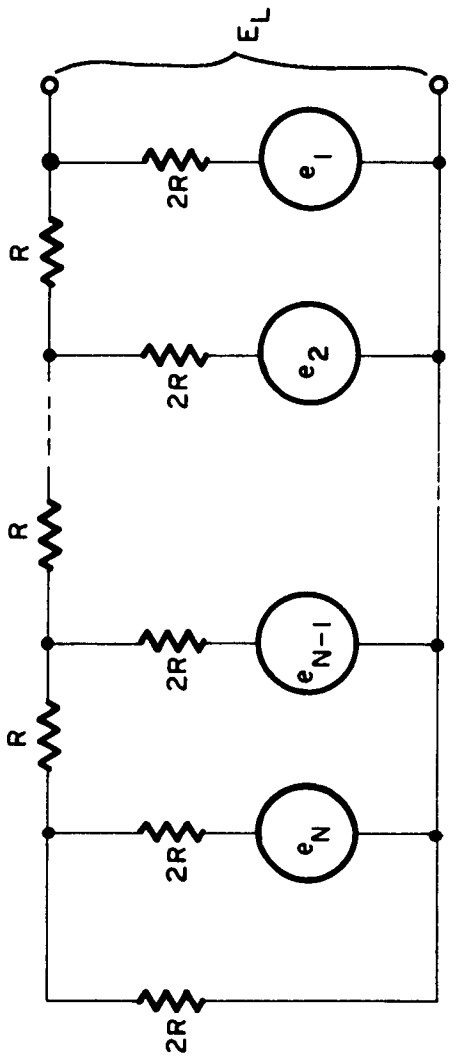

FIGURE 7: VOLTAGE-CONTROL LADDER CONVERTER

$$D_N = d_i \ 2^0 + d_2 2^1 + \text{---} + d_N 2^{(N-1)} \qquad (3)$$

Thus:

$$E_L = \frac{V_{ref}}{2^{(N)}} \quad D_N$$

Hence the ladder output is proportional to the binary number representing the voltage source conditions. If the sources were replaced by double-throw switches which selected either ground or a single reference source, then D_N would represent the condition of the switches.

A practical switch for such use is shown in Figure 8. Two reed relays replace the double-throw switch, one for ground and one for the reference source; because this arrangement gives less than one millisecond bounce time as opposed to about six milliseconds for a double-throw reed. The space and cost penalties for this speed are slight. The condition of the switch is determined as follows: An input of logical "one" saturates Q_1, energizing Coil 1. The combined collector load of the 600 ohm coil and the 1000 ohm resistor are sufficient to cause about a six volt drop across the 180 ohm resistor, which reverse-biases Q_2 and keeps it off. An input of logical "zero" holds Q_1 off, so that the four-volt base level of Q_2 causes it to conduct enough to energize coil 2. The two diodes and the 560 ohm

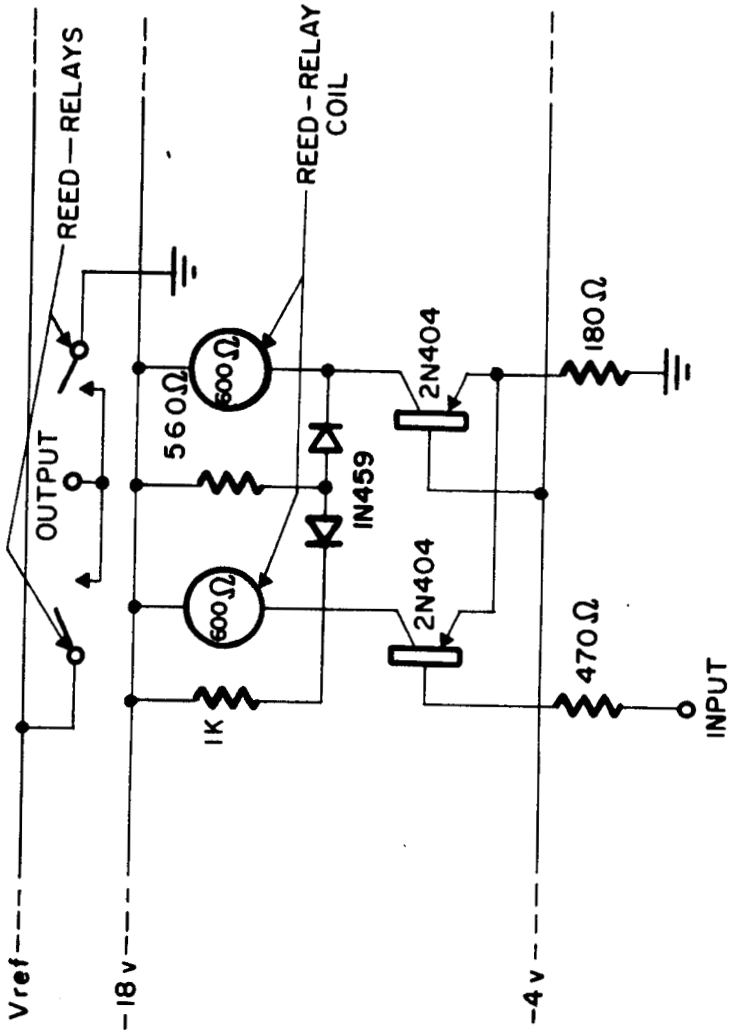

FIGURE 8: SWITCHED BINARY VOLTAGE SOURCE

resistor limit the inductive pulse when a coil is de-energized. Thus the binary value of the input determines whether the ladder source is zero or equal to the reference voltage. Note that it is conceivable that both reeds could briefly be closed simultaneously, shorting the reference source. The reference source must therefore incorporate current limiting.

Figure 9 shows the circuit of the ten-bit digital to analog convertor. The input requirements are compatible with the logic circuits used in the registers, and the ladder itself is indeed floating. Note that only one value of resistance is used in the ladder. This is because military surplus precision resistors were available for this purpose, a factor rewarding the choice of this type of convertor. In a ten-bit convertor, the final-stage resistors must have a tolerance of no more than plus or minus one-tenth per cent; involving considerable expense. The value of R used, 21,600 ohms, gives an output impedance of 10,800 ohms and permits conservative operation with a forty-volt reference. The left end termination shifts the zero reference by one-half bit, to permit balancing the bridge without the complete shorting of the potentiometer wiper to either side. The logic interface supplies power for the driving circuit.

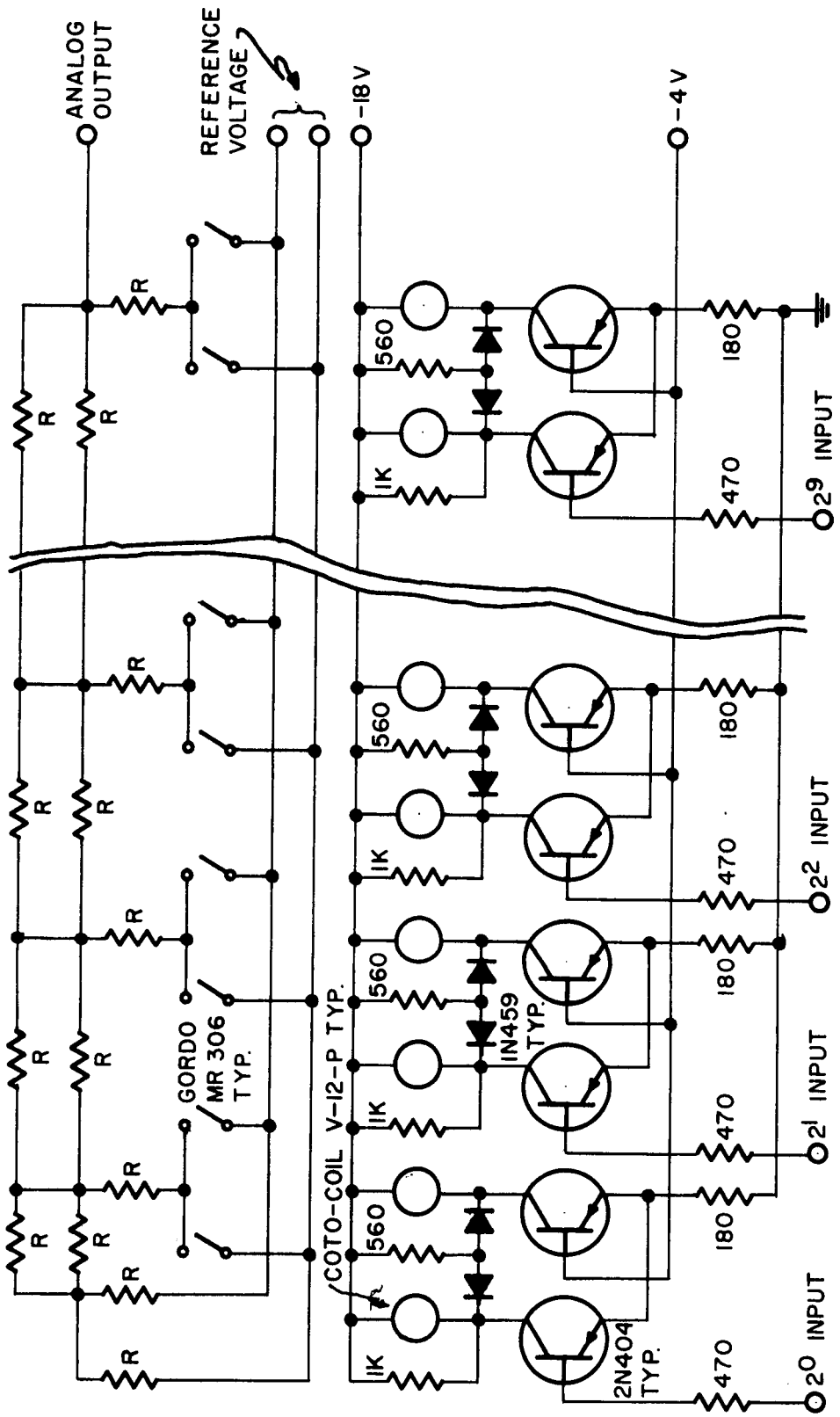

FIGURE 9: TEN-BIT DIGITAL-TO-ANALOG CONVERTER

Reference Voltage Source

The reference sources supplying the digital-to-analog convertors and the potentiometers are shown in Figure 10. The special transformer with seven secondaries permits the isolation required. The 1800 ohm resistor limits the current, and the Zener diode limits the voltage to thirty-nine volts. This value yields a reasonable sensitivity requirement (one bit equals forty millivolts), yet permits moderate impedance levels without large power dissipation. The potentiometers are 10,000 ohms, two-watt units, for example.

Bridge Connection

The connection of the potentiometer, reference source, and ladder convertor are shown in Figure 11. By equation (4), the voltage at the ladder, referred to the negative supply line, is:

$$E_L = \frac{V_{ref}}{2^{(N)}} D_N = \frac{39}{1024} (D_{10} + 1/2) \qquad (5)$$

The one-half is due to the ladder termination mentioned above. If the potentiometer angle is α and its maximum electrical travel is σ then its wiper voltage referred to the negative supply line is:

$$E_p = \frac{\alpha}{\sigma} V_{ref} = 39\frac{\alpha}{\sigma} \qquad (6)$$

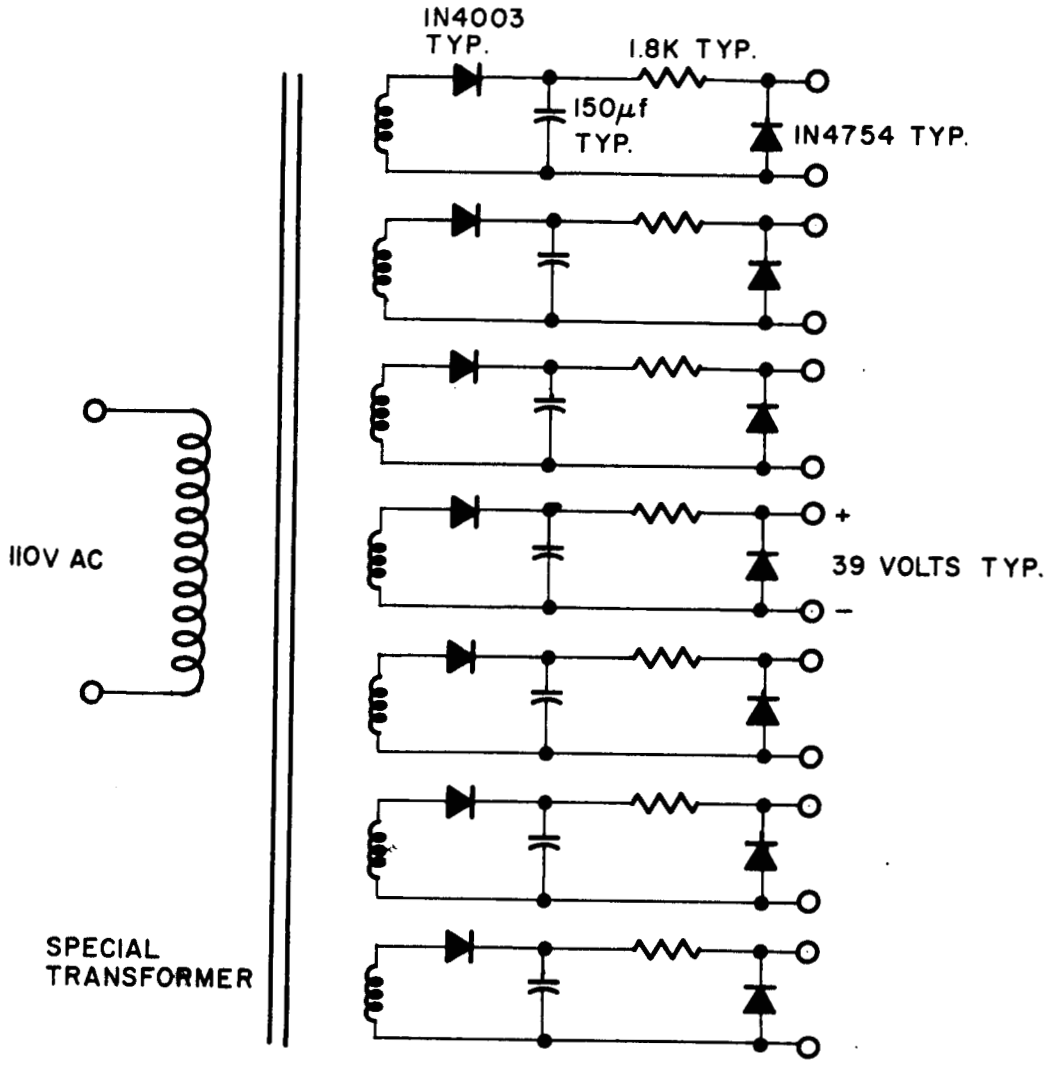

FIGURE 10: ISOLATED REFERENCE SUPPLIES

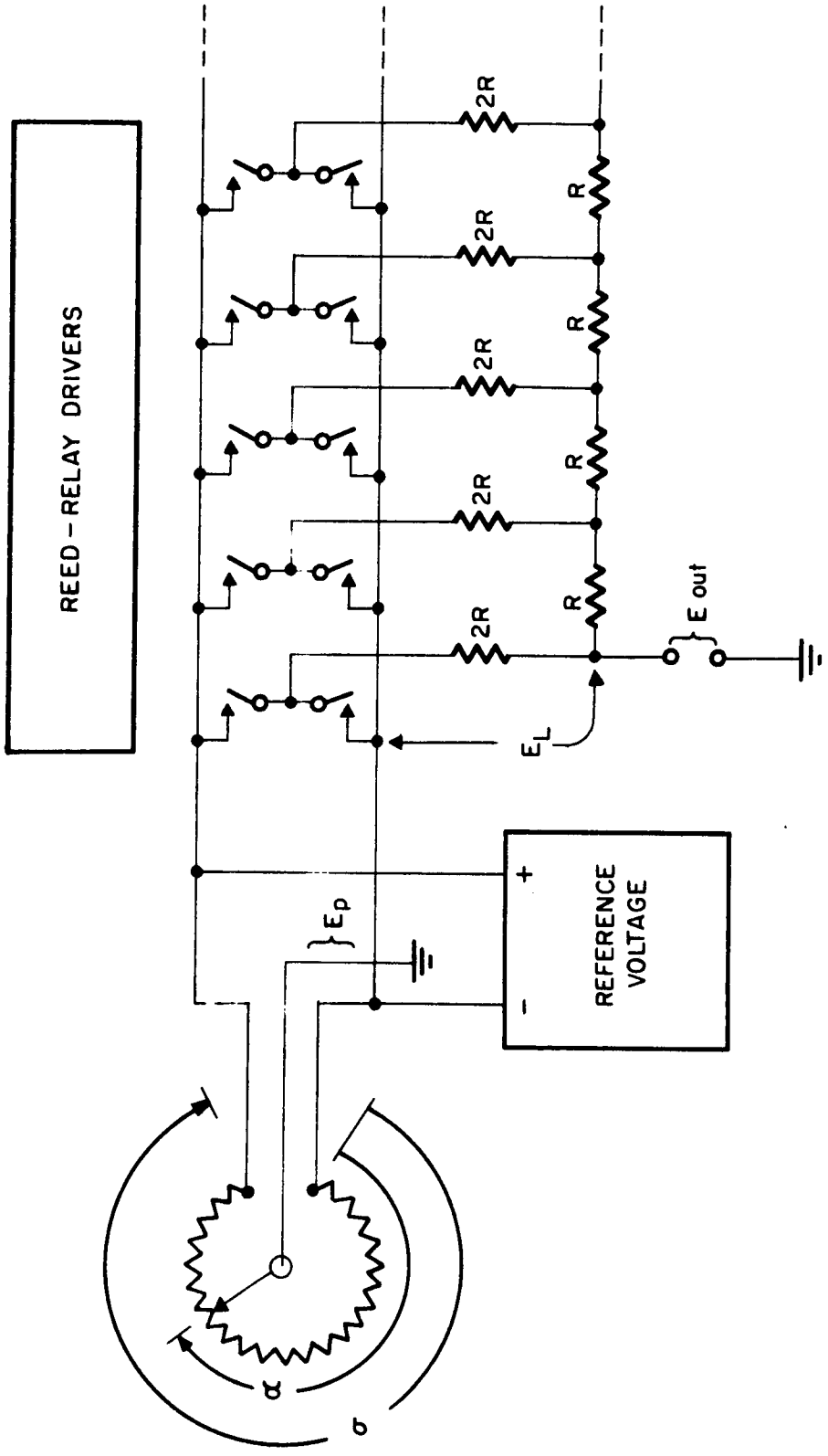

FIGURE 11: BRIDGE COMPARISON CIRCUIT

If the potentiometer wiper is grounded, the ladder output, referred to ground and unloaded, is:

$$E_L - E_P = V_{ref} \left| \frac{D_N}{2^{(N)}} - \frac{a}{\sigma} \right| \qquad (7)$$

$$E_{out} = 39 \left| \frac{D_{10} + 1/2}{1024} - \frac{a}{\sigma} \right| \qquad (8)$$

Thus balance occurs when:

$$a = \sigma \frac{D_{10} + 1/2}{1024} \qquad (9)$$

which is the desired condition.

The R. C. Active Filter

The choice of the filter configuration from the many documented[5, 6] depends on the design requirements other than the attenuation specifications. In this case, the requirements are:

1. The output impedance must be low to drive the servo-amplifier and null detector.
2. The source impedance varies from 10, 800 ohms to 13, 300 ohms due to the varying potentiometer output impedance.
3. The gain at D.C. is to be five.
4. The filter should not seriously load the bridge.
5. It should be simple enough to be an improvement over a passive (L.C.) filter with an amplifier.

The configuration which appears most amenable to these requirements is the unity-gain amplifier technique using one four-terminal R.C.[5] network. There are other techniques permitting higher gains[6], but they are inefficient in the use of elements. It was therefore considered preferable to modify (if possible) the unity-gain technique to permit higher gains.

The general circuit chosen is shown in Figure 12, together with its transfer function. With the gain set at five, experimentation produced these values:

$$g_1 = 1 \qquad C_1 = 1$$

$$g_2 = 1 \qquad C_2 = 2/5$$

$$g_3 = 1/2 \qquad C_3 = 1$$

The transfer function becomes:

$$T(s) = \frac{25}{4s^3 + 16s^2 + 9s + 5} \qquad (10)$$

The magnitude of this function on the imaginary axis is plotted in Figure 13, along with the normalized actual results obtained with ten per cent components. The peaking near an angular frequency of one-half permits a sharper cut-off and actually provides some lead compensation to the servo system.

The impedance level of the components was scaled up so that the variation in source impedance would have little effect

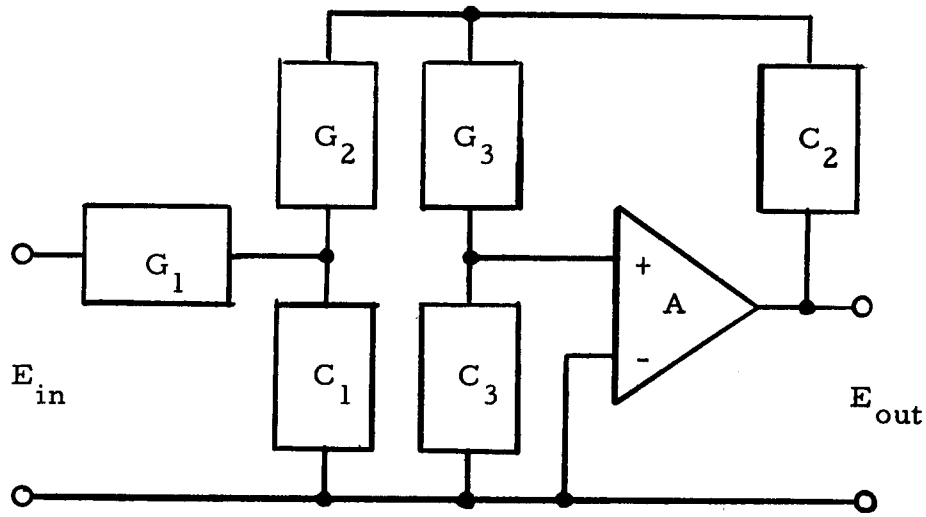

$$T(s) = \frac{E_{out}}{E_{in}} = \frac{AG_1G_2G_3}{Q} \quad ; \quad \text{Where Q is the function :}$$

$$Q = C_1C_2C_3s^3 + G_1G_2G_3 +$$

$$[\, G_1C_2C_3 + G_3C_2C_3 + G_2C_1C_3 + G_3C_1C_3 + (1-A)G_3C_1C_2 \,]\, s^2 +$$

$$[\, G_1G_2C_3 + G_1G_3C_3 + G_2G_3C_3 + G_2G_3C_1 + (1-A)(G_1G_3C_2 +$$

$$G_2G_3G_2)\,]s$$

FIGURE 12: R.C.ACTIVE FILTER PRINCIPLE

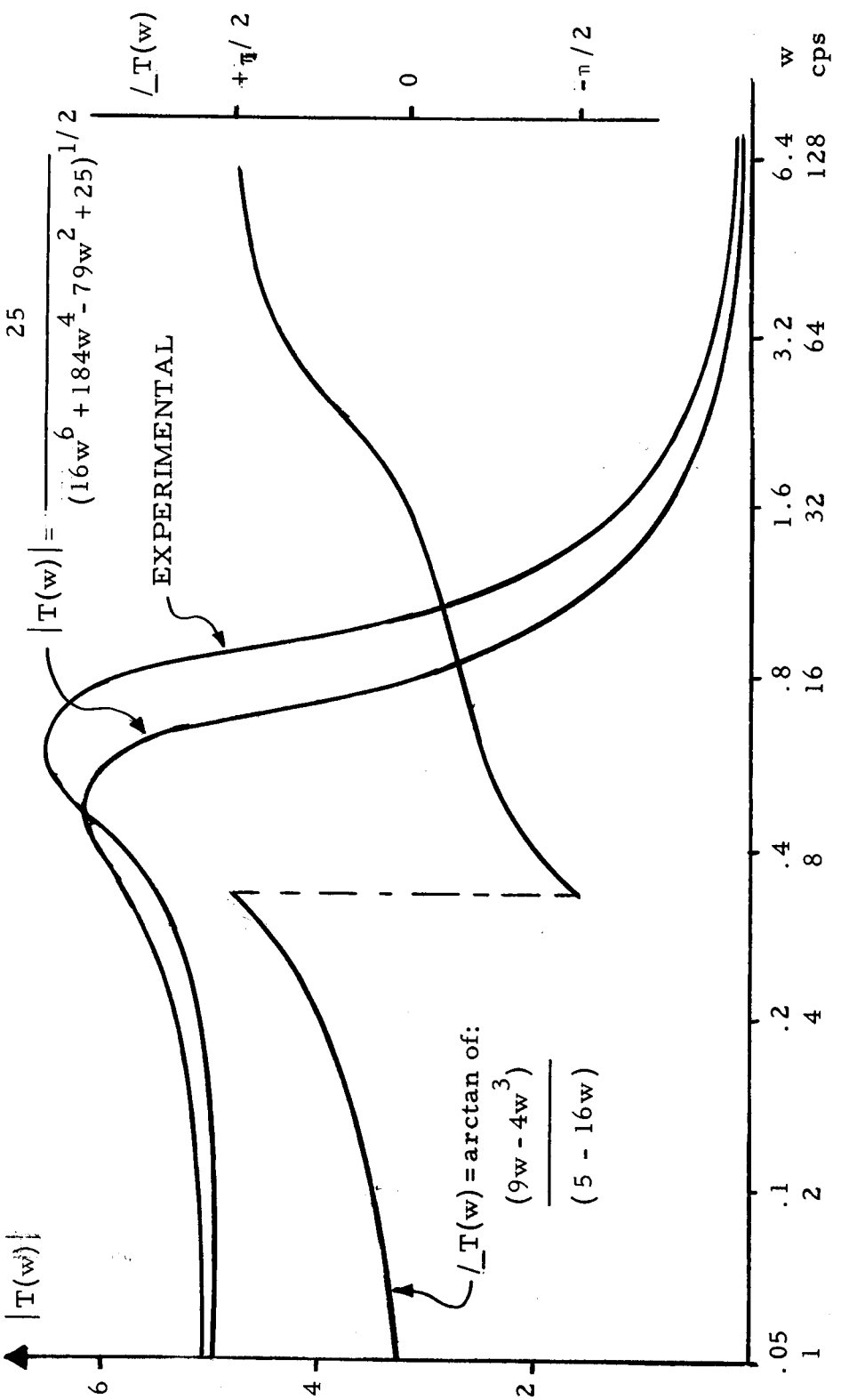

FIGURE 13: PHASE AND MAGNITUDE OF $T(s) = \frac{25}{4s^3 + 16s^2 + 9s + 5}$

on the filter (the equations assume zero source impedance). The frequency was then scaled to obtain cut-off at twenty cycles per second. The results, using standard values, are:

R_1 = 150, 000 ohms $\qquad$ C_1 = .05 micro-farad

R_2 = 150, 000 ohms $\qquad$ C_2 = .02 micro-farad

R_3 = 330, 000 ohms $\qquad$ C_3 = .05 micro-farad

The Operational Amplifier

The amplifier was assumed to have infinite input impedance and zero output impedance in calculating the transfer function. In addition, it must have very stable gain as this quantity affects the frequency response. It must also have a combined drift and off-set less than the forty millivolt system sensitivity desired. These requirements demand a design resembling operational amplifier techniques. The circuit developed is shown in Figure 14. To obtain the high input impedance field effect transistors (FET's) are employed in the first stage[7]. Silicon N-Channel FET's are used due to their exceptionally low offset current; and a matched pair, in a differential circuit and on a common heat sink, minimize the thermal drift. Balance is obtained by adjusting the 250 ohm trimmer. The 2N3368 FET is used because it is not expensive and was quickly available. The FET drains drive

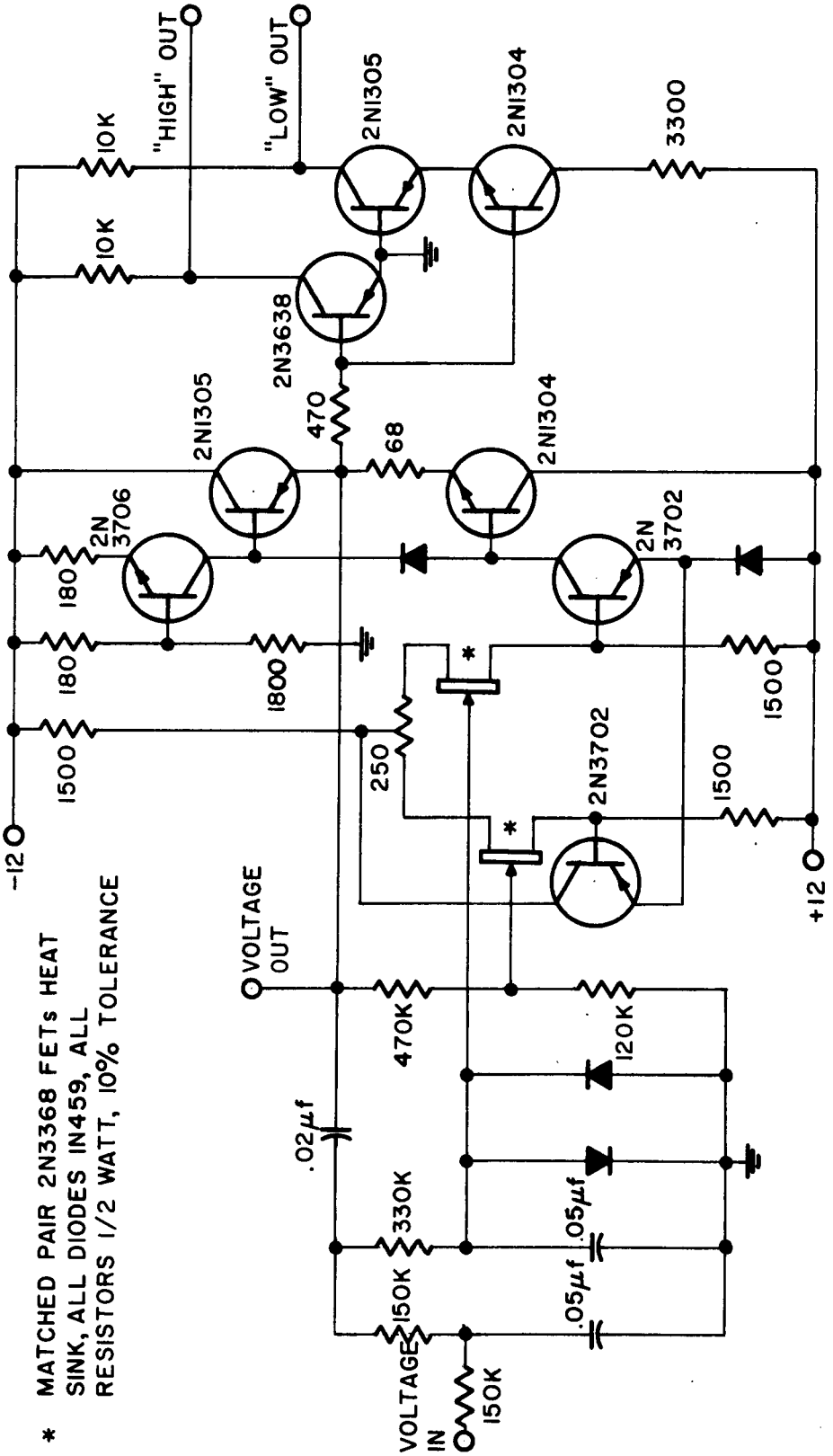

FIGURE 14: R.C. ACTIVE FILTER SCHEMATIC

a pair of 2N3702 transistors directly to minimize changes in drain current. One of these transistors drives the FET's source resistor to improve the common mode rejection; the other drives the output through the complementary emitter follower consisting of the 2N1304 and 2N1305 transistors. The 2N3706 acts as a current source load to increase the gain and voltage swing. This amplifier has a gain near 2000 but is stable under heavy feedback. The divider formed by the 470, 000 ohm and 120, 000 ohm resistors holds the gain stable at nearly five by feedback to the negative input, and reduces the output impedance considerably. Since an FET can be injured by excessive gate voltage, and the bridge is capable of producing forty volts; the back-to-back diodes hold the input to plus or minus seven-tenths of a volt. Because they follow the filter elements they cannot introduce error by rectifying noise.

The Null Detector

The null detector is also shown in Figure 14. Its function is to ground a "high" error line if the filter output is more than slightly positive, and to ground a "low" error line if it is more than slightly negative. In brief, it consists of a complementary pair of greatly over-driven amplifiers, with an invertor (2N1305) in series with the NPN (2N1304) to provide negative voltage on

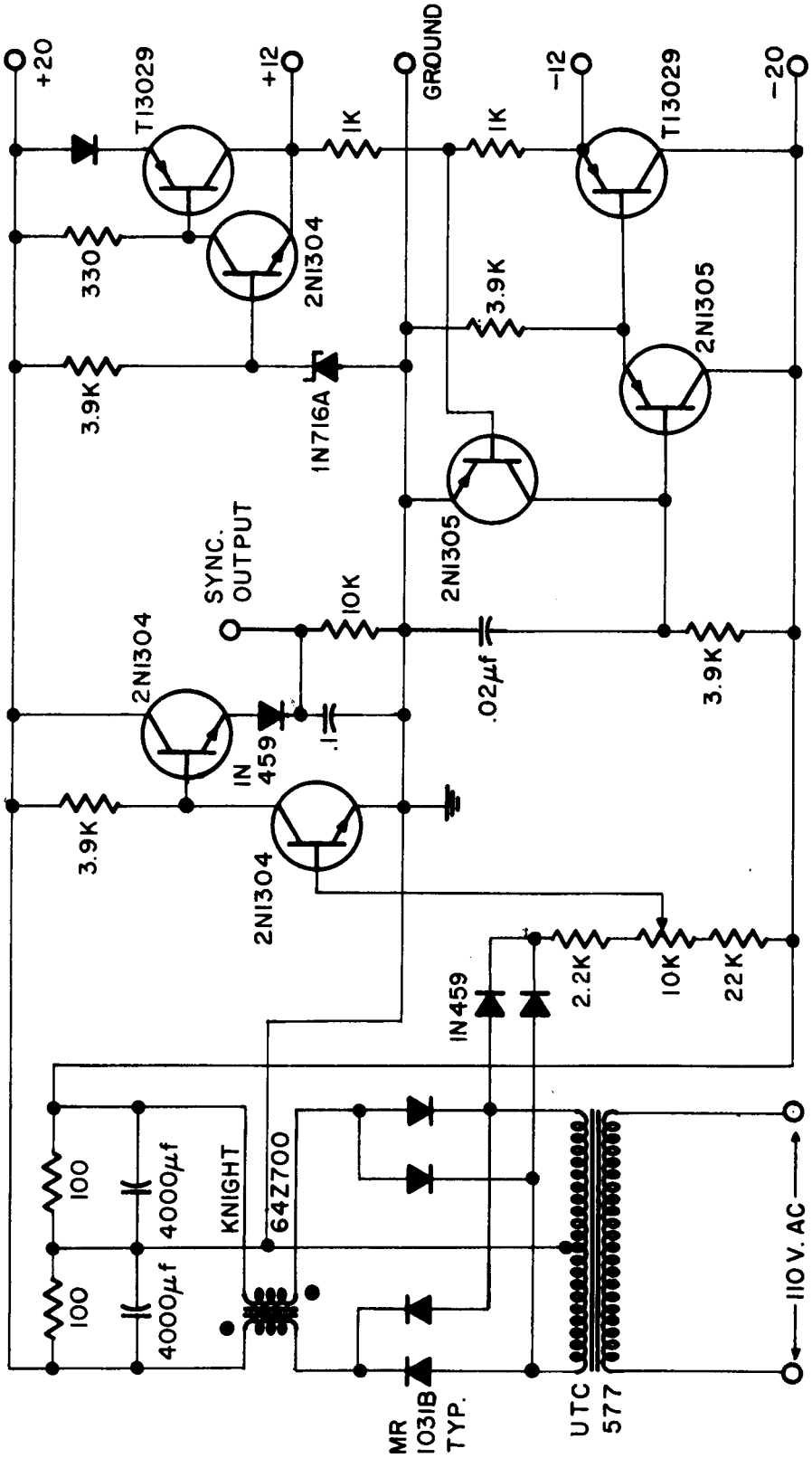

FIGURE 15: DATA CONVERSION POWER SUPPLY

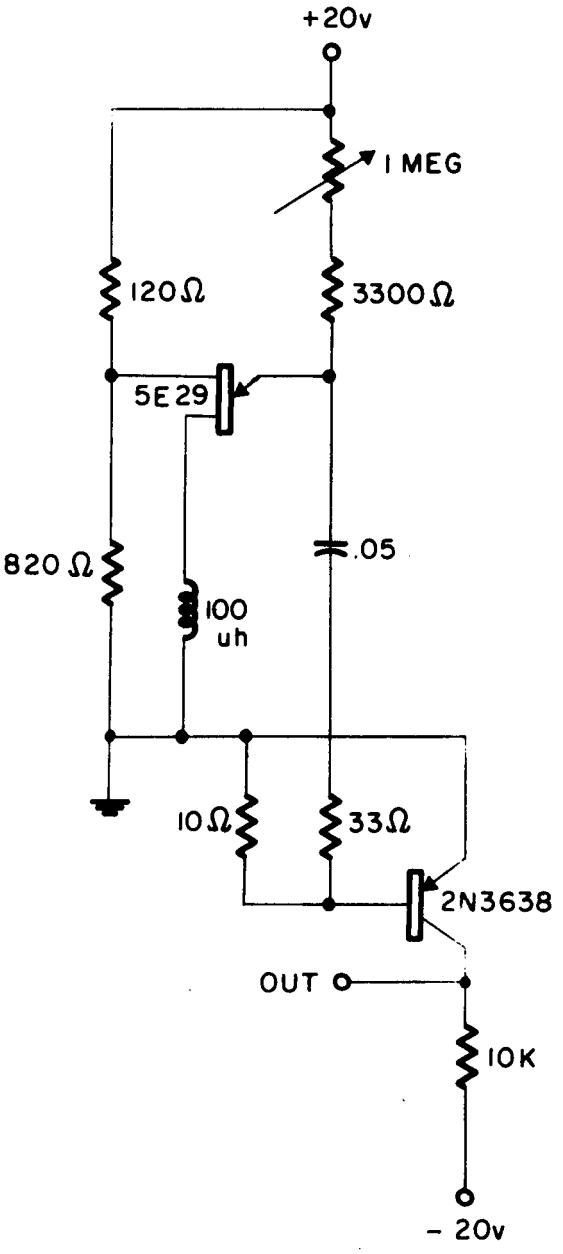

FIGURE 16: TRACKING OSCILLATOR

CHAPTER IV
THE DRIVE SYSTEM

Basic Principle

As implied in Chapter II, the servo-amplifiers drive series-would D.C. motors by phase-switching the sixty-cycle A.C. line. Figure 17 shows the connection of the output stage to the motor. When SCR's 1 and 2 are switched on, point A is driven positive and current flows through the motor by the route A-B-C-D. When SCR's 3 and 4 are switched on, point B is driven negative and current flows through the motor by the route D-C-A-B. Thus the armature current may be reversed without reversing the field current, reversing the torque of the motor.

Advantages

The circuit of Figure 17 has a number of advantages for this application. It requires a near minimum of two wires per motor, plus a ground return common to all motors; to be run between the amplifiers and the motors on the manipulator. The only electronic components which must be mounted at the motor are the two diodes. The SCR's provide a very efficient, simple, low-impedance, and high-gain output stage. The connection of

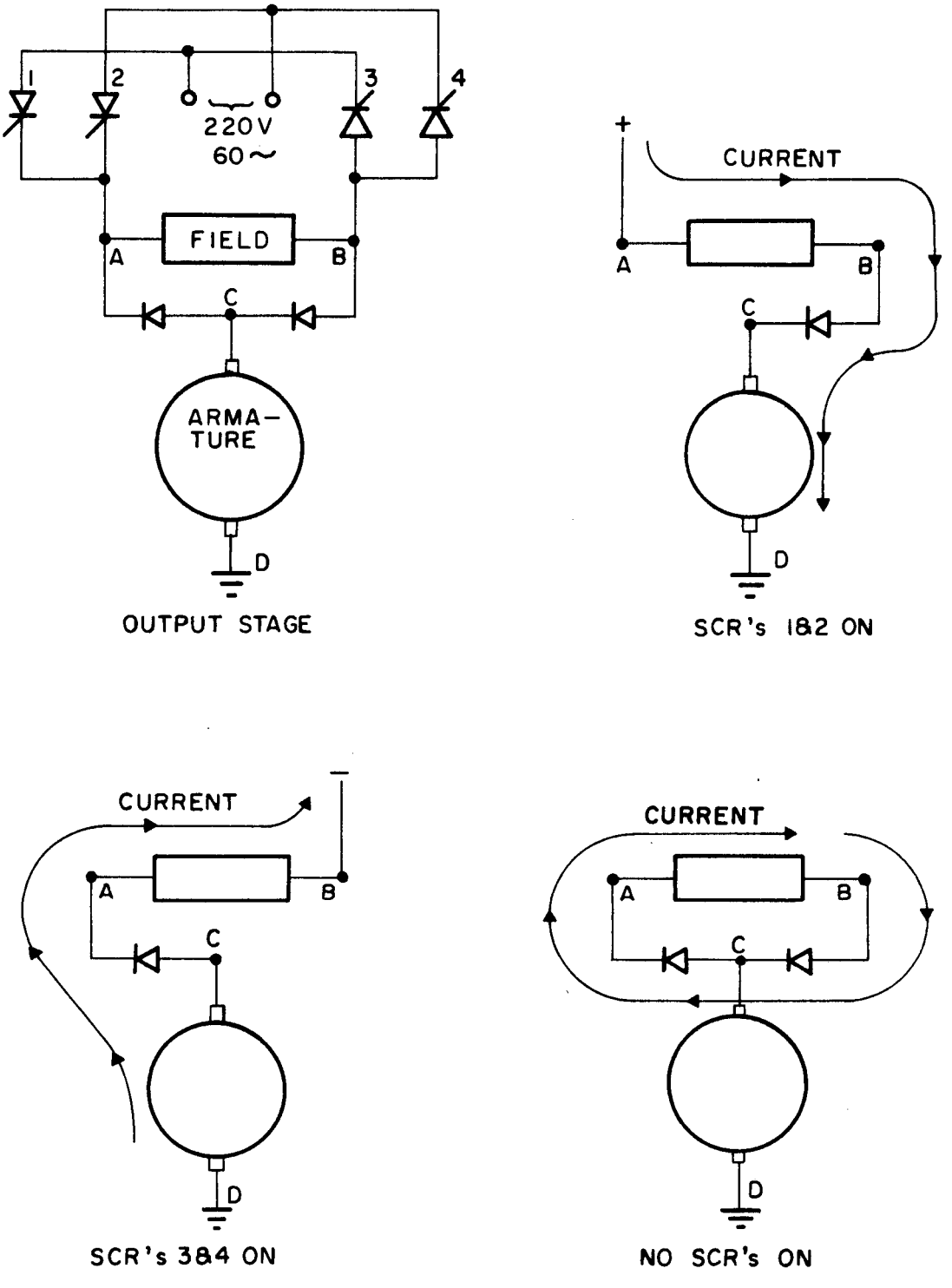

FIGURE 17: BASIC MOTOR-DRIVE CIRCUIT

the motor field between points A and B limits the fault current if forward and reverse drives should appear simultaneously, and the natural commutation of the SCR's also contributes to the reliability. As will be shown, the circuit also permits simple and elegant methods of rate damping, slew limiting, and friction compensation.

Proportional Control

Since the SCR is a switching device, the mean output of the amplifier can be varied only by varying the phase angle of the A.C. power at which the SCR's are switched on. This is accomplished by providing a syncronous pulse train to the appropriate SCR's. When the gate of an SCR is pulsed, it will switch on if its anode to cathode voltage is positive and remain on until the progress of the sinusoidal input reverses that voltage. Figure 18 illustrates the wave forms resulting from this method of control. The average and peak values of this wave form are:

$$V_{ave} = \left| \frac{M}{\pi} (1 + \cos \phi) \right| \quad 0 \leq \phi \leq \pi \qquad (1)$$

$$V_{peak} = \begin{cases} M \text{ for } 0 \leq \phi \leq \pi \\ M \sin (\pi - \phi) \text{ for } \pi/2 \leq \phi \leq \pi \end{cases} \qquad (2)$$

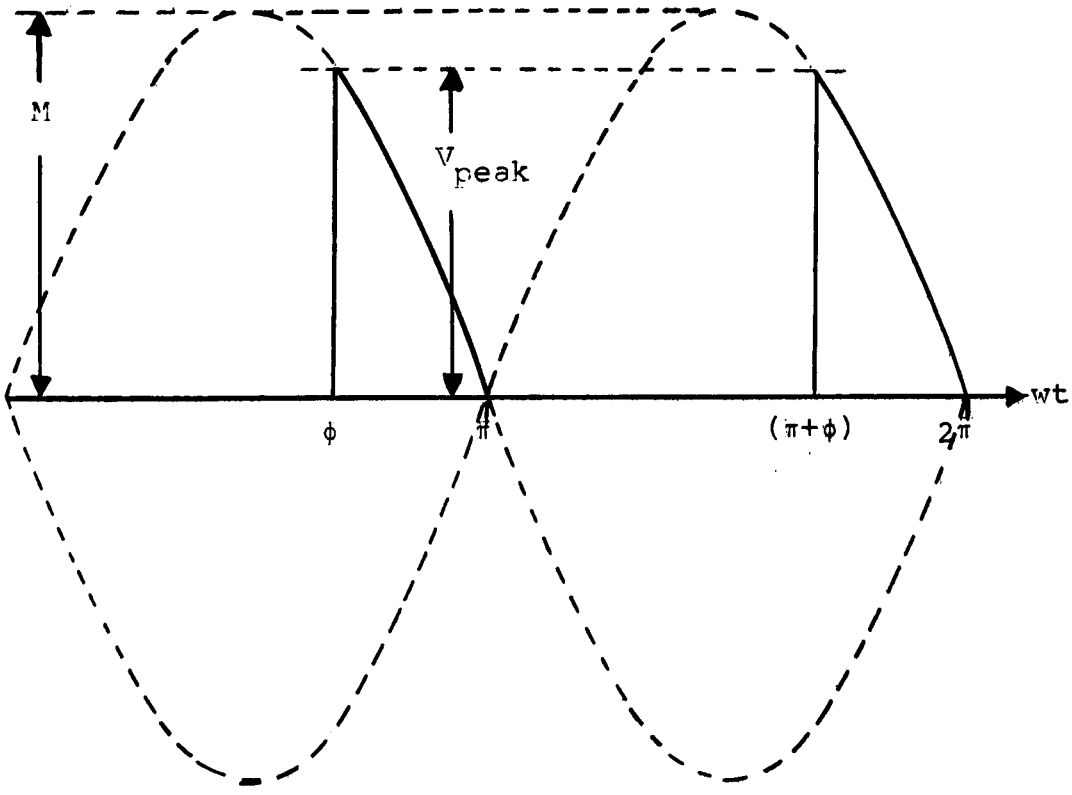

$$V_{ave} = [M/\pi(1 + \cos\phi)]_{0 \leq \phi \leq \pi}$$

$$V_{peak} = \begin{cases} M \text{ for } 0 < \phi < \pi/2 \\ M \cdot \sin(\pi - \phi) \text{ for } \pi/2 \leq \phi \leq \pi \end{cases}$$

FIGURE 18: IDEAL PHASE SWITCHING WAVEFORMS

Series Motor Characteristics

The amplifier design depends on the behavior of a series motor under such a drive. The basic equations of a series motor are [8]:

$$T = \frac{AV^2}{(N + BR)^2} = KI^2 \qquad (3)$$

Where A, B, R, and K are motor constants.

Rearranging:

$$|V/I| = K/A\,(N + BR) \qquad (4)$$

These equations are plotted in Figure 19. It is clear that during plugging (rapid deceleration) there is a critical speed N_c at which the motor impedance vanishes; that is, $N_c = -BR$. If the voltage source is stiff, as is an SCR controller; a theoretically infinite current will flow and produce an infinite torque. This will instantly decelerate the motor until $|N_c| < BR$. In practice an infinite current is impossible, principally due to the field inductance; but a sudden voltage reversal can be accompanied by a large current pulse if the speed exceeds N_c. Where this is possible, the critical speed can be increased by adding a small series resistor.

In equations (3) and (4), V represents the average voltage. During stall this may be taken as V_{ave} of equation (1) when

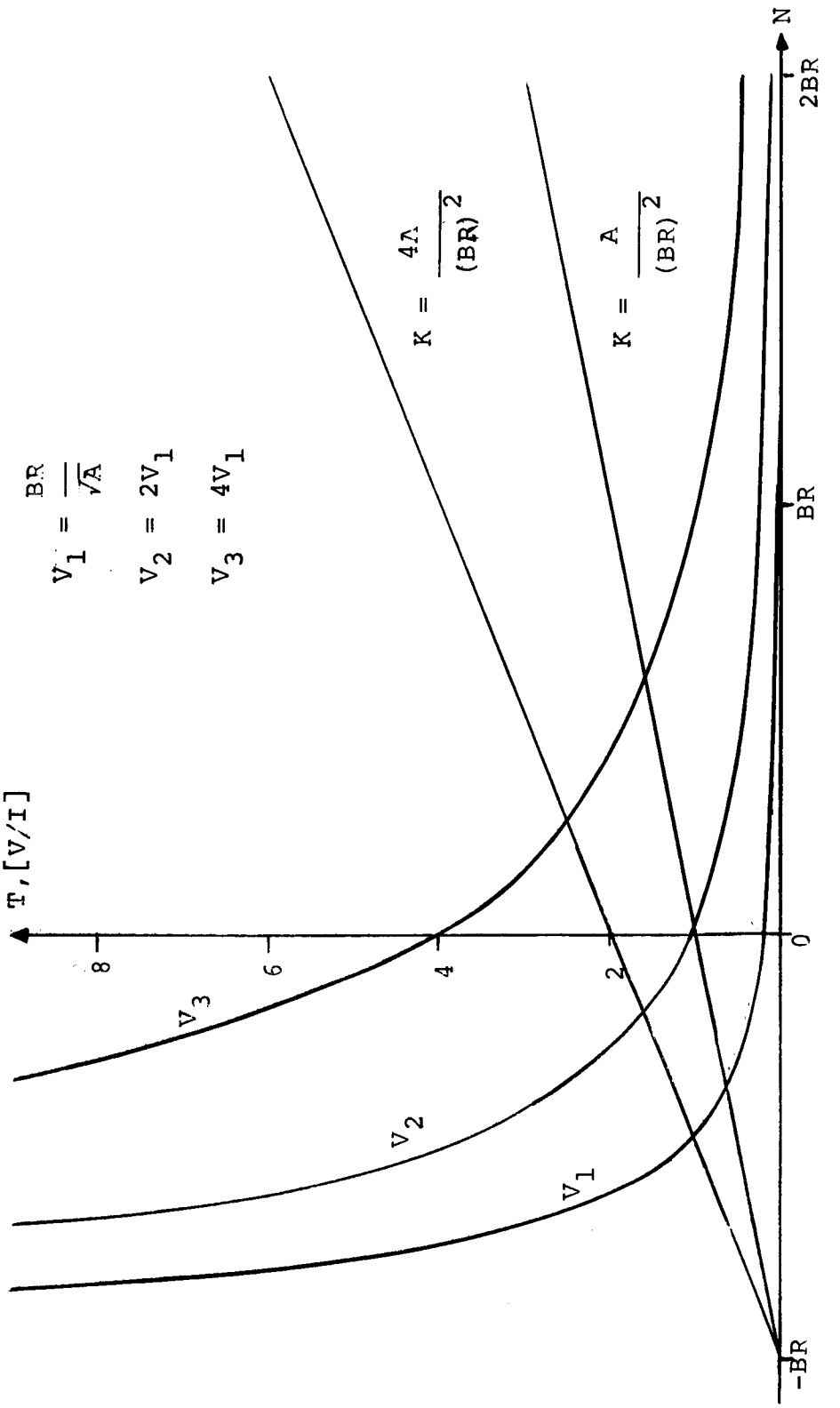

FIGURE 19 SERIES MOTOR CHARACTERISTICS

operating from an SCR controller, but when the motor speed is not zero the armature E.M.F. will back-bias and commutate the SCR's at a phase angle other than π. Thus by coasting between power pulses the motor raises the effective average voltage. Under light torque loads, then, the armature E.M.F. can approach V_{peak}; so that for small values of ϕ in equation (1) the SCR will be back biased when the pulse occurs (the E.M.F. will exceed the instantaneous line voltage). In this condition the motor speed will pulsate; that is the speed will increase as if the input were nearly V_{peak} until the E.M.F. blocks the SCR firing, it will then decay down until firing resumes. Since the power pulses are large for small values of ϕ, one or two pulses will accelerate the motor speed considerably, requiring several cycles to decay back to the speed at which firing resumes. The E.M.F. is sustained because the field current can circulate between SCR conductions by returning from B to A through the diodes (see Figure 17). Since the field inductance is appreciable, the flux in the motor air-gap may decrease as slowly as the armature speed does. If this pulsation condition is intolerable it must be avoided.

Combined Characteristics

The preceding ideas are illustrated in Figure 20. The

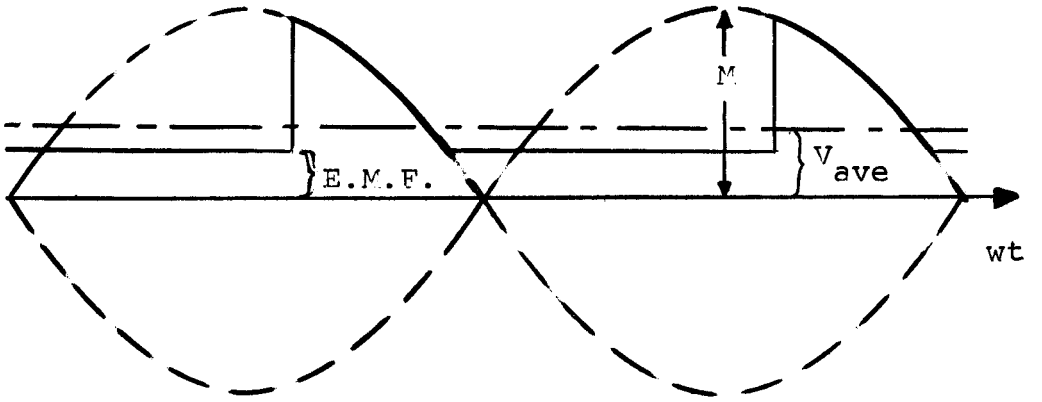

Infinite Inductance

$$E.M.F. = \sqrt{K/ENI} = N\sqrt{T/A}$$

$$V_{ave} = \frac{M}{\pi}[\cos\phi + E.M.F.(\phi + \sin^{-1}\frac{E.M.F.}{M}) + \sqrt{1-E.M.F./M}]$$

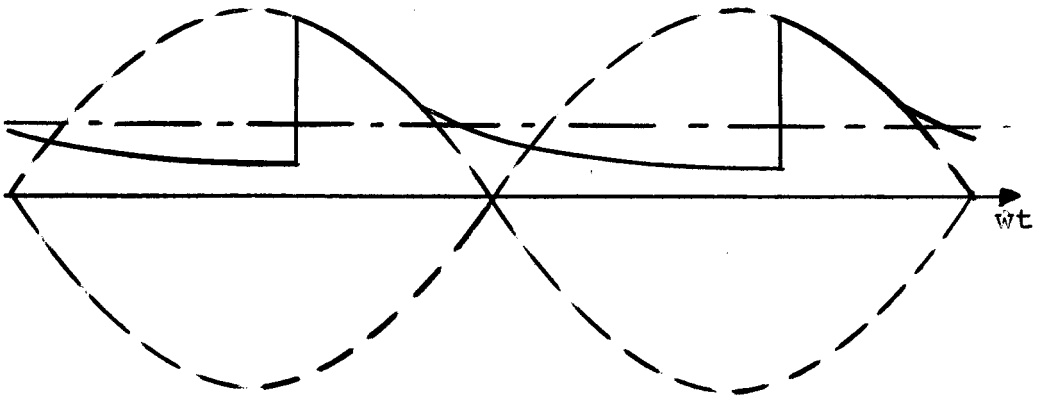

Finite Inductance

FIGURE 20: ACTUAL SWITCHING WAVEFORMS

armature E.M.F. is proportional to the product of the speed and the instantaneous field current. If the field inductance is zero the field current will always equal the SCR current, and commutation will occur at a phase angle of π. In this case equation (1) applies. At the opposite extreme, an infinite field inductance will hold the E.M.F. constant at steady state, and V_{ave} can be computed as indicated. For finite values of field inductance, the steady-state E.M.F. will decay between power pulses due to the field resistance and the diode drops, and some intermediate value of V_{ave} will occur. For a positioning system the exact behavior is usually of interest only near the null, then N is small and equation (1) may be used. It might be desirable to compute the high-speed E.M.F. to determine what value of phase angle will produce pulsating, but experience has shown that with realistic loads the value is small enough that clamping ϕ to be above that value involves little performance penalty. As will be shown, such clamping is simply obtained.

Pulsing Requirements

We are now able to define the requirements for the pulse generator that fires the SCR's. As seen in equation (1), the servo amplifier's output is maximum for a phase angle (ϕ) of zero; and diminishes with increasing ϕ until at $\phi = \pi$ the output is zero.

Thus with a maximum (saturated) positive input, the pulse generator should produce pulses only in the forward SCR's at a minimum phase angle limited to the pulsating value discussed above. As the input decreases, ϕ should increase until at no input $\phi = \pi$. As the input goes negative, the pulses should be shifted to the negative SCR's, and ϕ should diminish until at minimum input (negative saturation) the phase angle is again clamped at its minimum value. Furthermore, some provision to prevent both a forward and a reverse SCR being fired during the same half cycle of the line voltage should be made. This could happen otherwise if the input changed rapidly.

Pulse Generation Principle

Figure 21 shows the block diagram of such a pulse generator. The input drives a differential amplifier which produces symetrically opposed outputs. These outputs control current sources whose outputs are integrated by capacitors. Level detectors monitor the capacitors and trigger one-shot pulse generators. Each of these generators trigger the appropriate set of SCR's. The bias current of the differential amplifier is used to set the common level of the outputs with no input so that the integration delay corresponds to $\phi = \pi$. If these outputs are unbalanced by an input one capacitor will charge

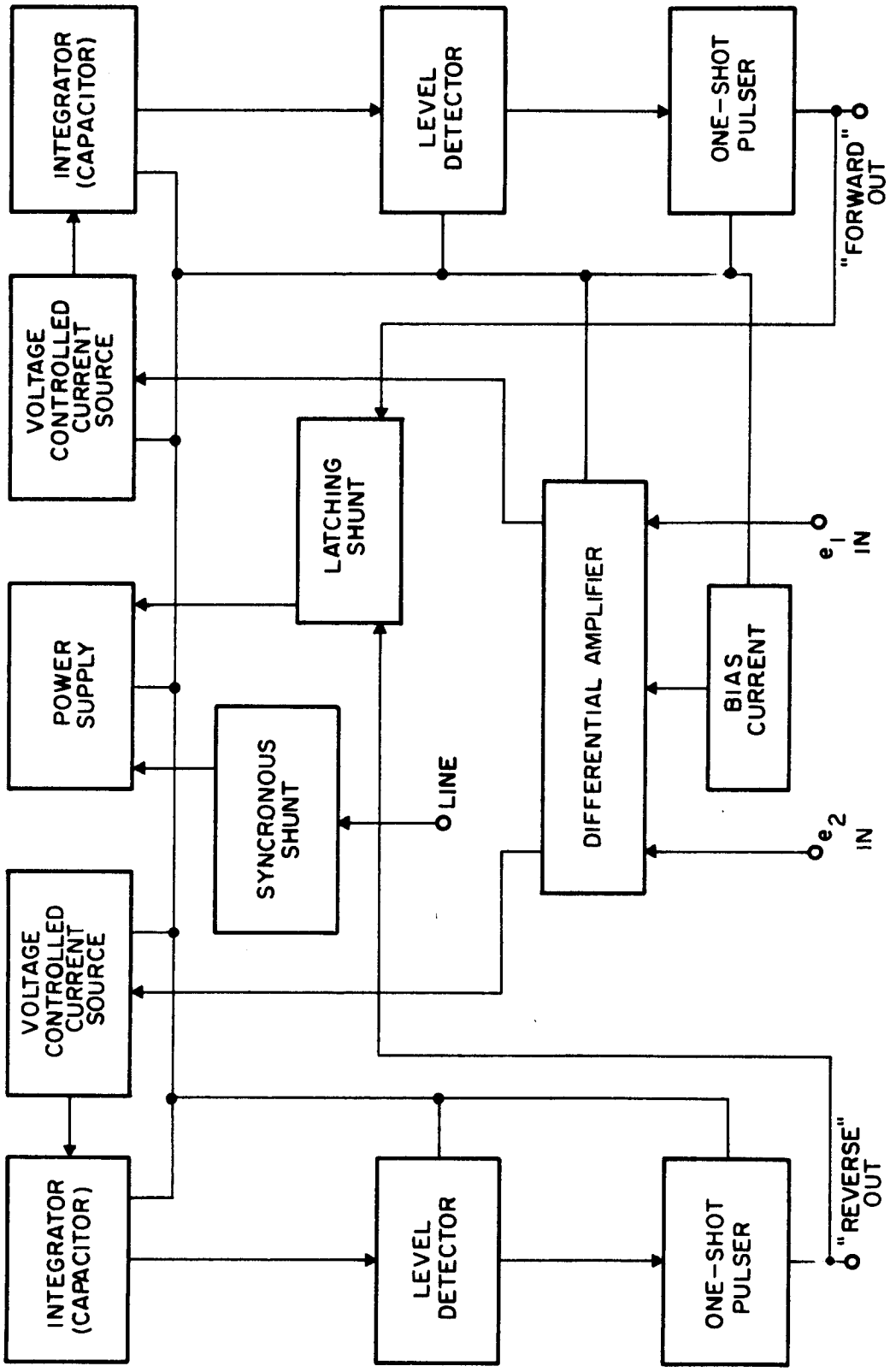

FIGURE 21: PULSE GENERATOR BLOCK DIAGRAM

faster and the other more slowly. Which ever one-shot triggers first sets the latching shunt to short out the power supply, preventing further pulses. It also discharges the capacitors. A syncronizing shunt also shorts the supply at the end of each half cycle. This opens the latching shunt, or, if it was open, discharges the capacitors; so that when the syncronizing shunt opens the next control cycle begins. By varying the duration of the syncronizing shunt, the phase of the earliest possible pulse can be determined (since it cannot occur before the shunt opens). This feature is used to set ϕ_{min} to prevent pulsating.

Refinements

This system permits several refinements. By increasing the bias current to the differential amplifier, the no-input value of ϕ can be reduced to be less than π. This means that as the input decreases from positive saturation, the SCR output (V_{ave} in equation (1) will decrease to some finite value when the input reaches zero. As the input goes negative, V_{ave} will jump to the equivalent negative value, as the pulses are transfered to the reverse SCR's; and more negative inputs will reduce and cause more negative values of V_{ave}. This property has the effect of giving the servo amplifier negative deadband and can be used to cancel the motor deadband by avoiding the low voltages

at which friction is greater than the motor torque.

A second refinement permits damping feedback to be taken directly from the armature of the motor, without a separate tachometer. The equations of Figure 20 show that the E.M.F. is proportional to the field current and to the speed of the armature. After an SCR is pulsed and is conducting armature current flows and the attendant I-R drop obscures the E.M.F. at the armature terminals. However, when no SCR is conducting there is no armature current. Furthermore, the field current is circulating through the diodes, so that they are forward biased and have small voltage drops. Thus the E.M.F. is available at the servo-amplifier without running extra wires by averaging the voltages at A and B (see Figure 17.) Conversely, due to the action of the latching shunt the pulse generator reacts to inputs only before an SCR is pulsed. Thus the two output lines may be averaged with a resistive divider and applied to the negative input of the differential amplifier. Despite the current or torque dependence of the velocity feedback so obtained, the damping appears to be satisfactory in moderate-gain systems.

Analysis

We can now derive a transfer function for the complete servo-amplifier. In Fgiure 21, the outputs of the voltage

controlled current sources will be:

$$i_1 = g(e_1 - e_2) + ki_o$$
$$i_2 = g(e_2 - e_1) + ki_o \qquad (5)$$

The time required for the capacitor voltages to reach the trip-point of the level detectors is given by:

$$e_f C = \int_0^{T_1} i_1 \, dt \qquad e_f C = \int_0^{T_2} i_2 \, dt \qquad (6)$$

or, if i_1 and i_2 are assumed constant:

$$T_1 = \frac{e_f C}{i_1} \qquad T_2 = \frac{e_f C}{i_2} \qquad (7)$$

The phase angles resulting from these delays and T_0, the delay due to the syncronizing pulse, are:

$$\phi_1 = w(T_0 + T_1) \qquad \phi_2 = w(T_0 + T_2) \qquad (8)$$

Combining these results with equation (1), we have for $e_1 \geq e_2$:

$$V_{ave} = \frac{M}{\pi} + 1 + \cos\left(wT_0 + \frac{we_f C}{g(e_1 - e_2) + ki_0}\right)$$

and for $e_2 \geq e_1$: (9)

$$V_{ave} = -\frac{M}{\pi} \left| 1 + \cos\left(wT_0 + \frac{we_f C}{g(e_2 - e_1) + ki_0}\right) \right|$$

These equations are plotted in Figure 22. Note that when:

$$i_0 = \frac{e_f C}{k(\pi/w - T_0)} \qquad (10)$$

There is no discontinuity in control, but that otherwise there is a deadband, referred to the input, of:

$$D.B. = \frac{2\, e_f C}{g(\pi/w - T_0)} - \frac{2k}{g}\, i_0 \qquad (11)$$

Clearly, this deadband can be negative.

Side-Effects

It should be noted that with negative deadband as described there will be power dissipated in the motor even with no input. This is avoidable by advancing the turn-on of the syncronizing shunt until it just deletes the no-input pulses. However, since all seven servo-amps are syncronized from the same source, in practice the shunting time is set at a compromise value and all the pulse generators are set so that their no-input pulses are deleted.

Like any sampling amplifier, the SCR driver is susceptible to syncronous noise. When input noise is present then i_1 and i_2 cannot be assumed constant in equation (7), and equation (6) must be used. It is seen that many sinusoidal signals imposed on i_1 and i_2 could vary T_1 or T_2, but that only those at multiples

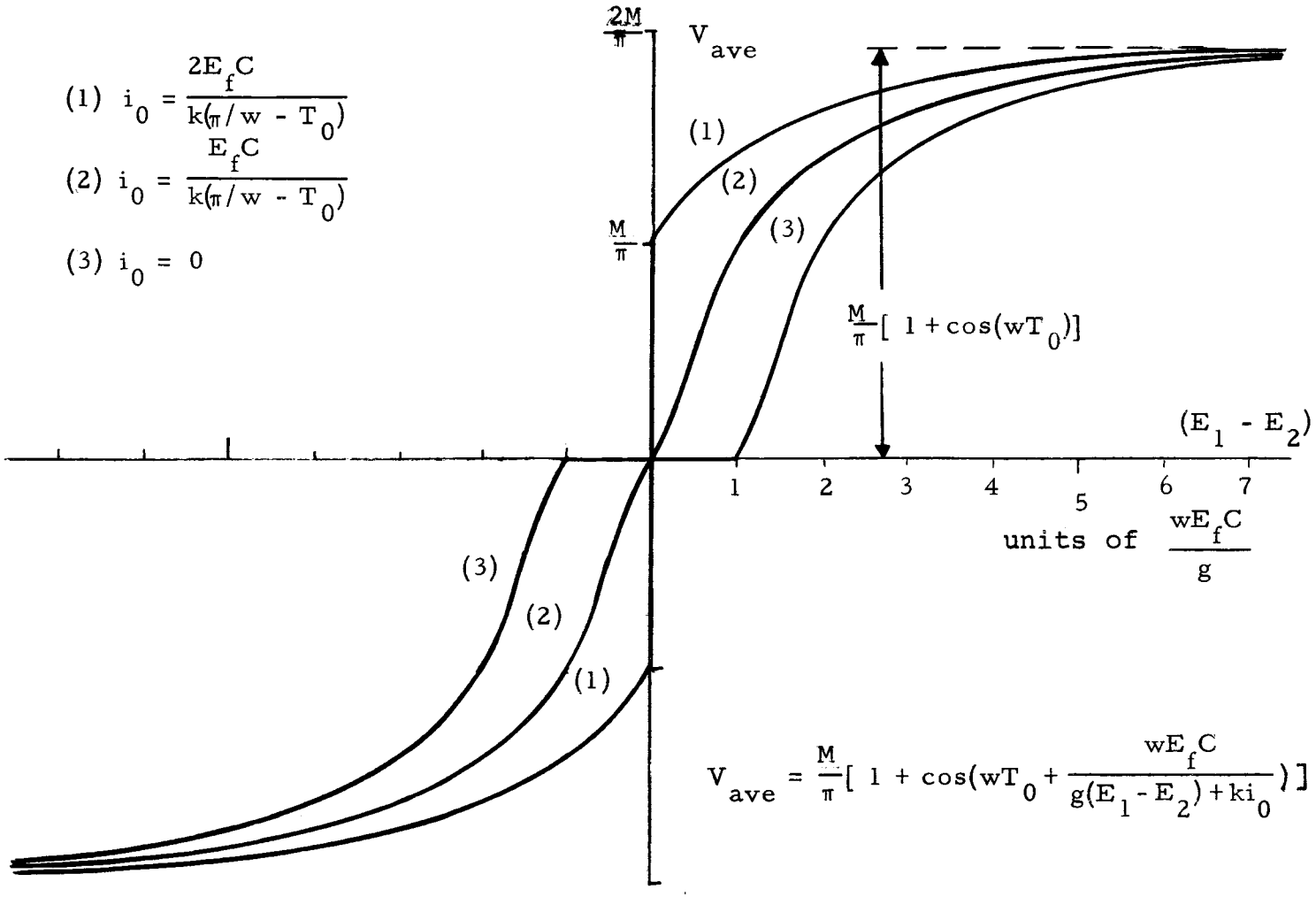

FIGURE 22: SCR DRIVE AMPLIFIER CHARACTERISTICS

of the sampling rate (120 cps.) could produce an accumulative effect over many cycles. Unfortunately, this is exactly the type of noise generated by the phase-switched SCR's. Hence the need for a low-pass filter is illustrated.

Circuit Details

Figure 23 shows the pulse generator. The two 2N3704 transistors form the differential amplifier, and were chosen for their low cost and low drift with temperature. The bias current is set by adjusting the 50k reostat. The voltage controlled current sources are the 2N3638 transistors, also chosen for low drift and cost. They share a common emitter resistor to improve the differential gain. The functions of level detector and one shot are performed by the 5E29 unijunction transistors, which are coupled to the SCR's through pulse transformers. The latching shunt is a composite complementary switch consisting of the cross-coupled 2N1304 and 2N1305, and is turned on by either unijunction through the 1000 ohm resistors. The 1N459 diodes then discharge the timing capacitors. The remaining 2N1304 is the syncronizing shunt, and is driven by a circuit in the power supply. The RC networks supplying the upper base of each unijunction prevent interactions, and the 47 ohm resistor and one-tenth micro-farad capacitor prevent junction

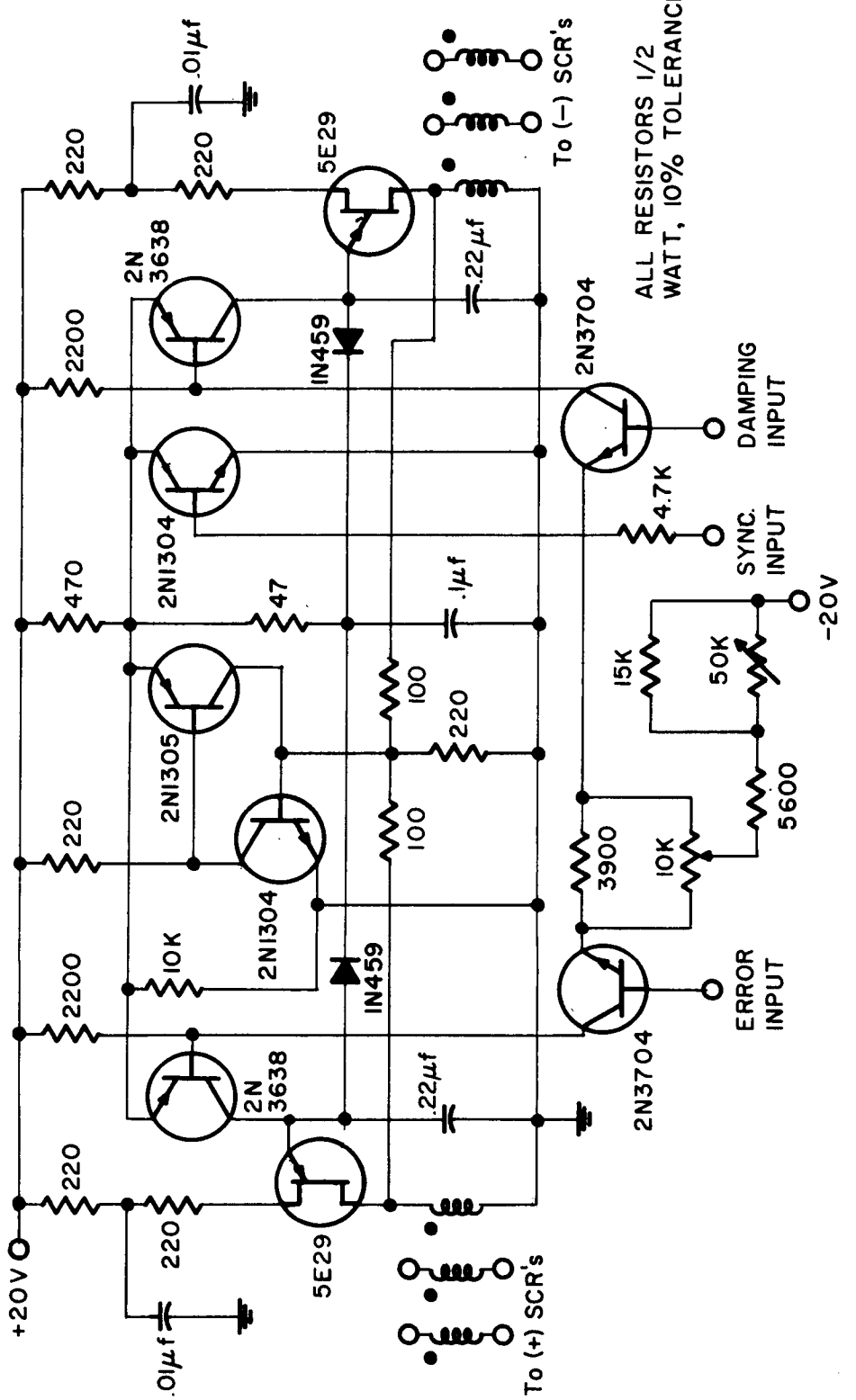

FIGURE 23: PULSE GENERATOR SCHEMATIC

capacitances in the latching shunt from causing turn-on.

The common power supply was shown in Figure 15. Little comment is required except to observe that the width of the positive-going syncronizing pulse can be varied by the 10K potentiometer.

The SCR output stage of the servo-amplifier is shown in Figure 24. The 2N3898 SCR is conservatively rated and fairly inexpensive. The damping signal is obtained as described and can be varied by the 100Kpotentiometer. The connection of the motor shows the use of slew limit switches with dynamic braking. When, for example, the forward limit switch is opened the forward SCR's are disconnected and the reverse input grounded through an auxiliary diode and resistor. This effectively imposes the E.M.F. across the field in a direction to cause regeneration and a rapid stop. The use of the diode permits the reverse drive to be employed in a normal way. Only five controlled axes on the manipulator have limit switches, and only the hoist has dynamic braking; but the omissions are obvious.

Figure 25 shows the manual control potentiometers and the manual-automatic input selector. Two relays were used to obtain the necessary number of poles; they are driven in parallel by the 2N3638 transistor from a control signal produced by the inter-face logic. The 2, 200 ohm resistors insure that during

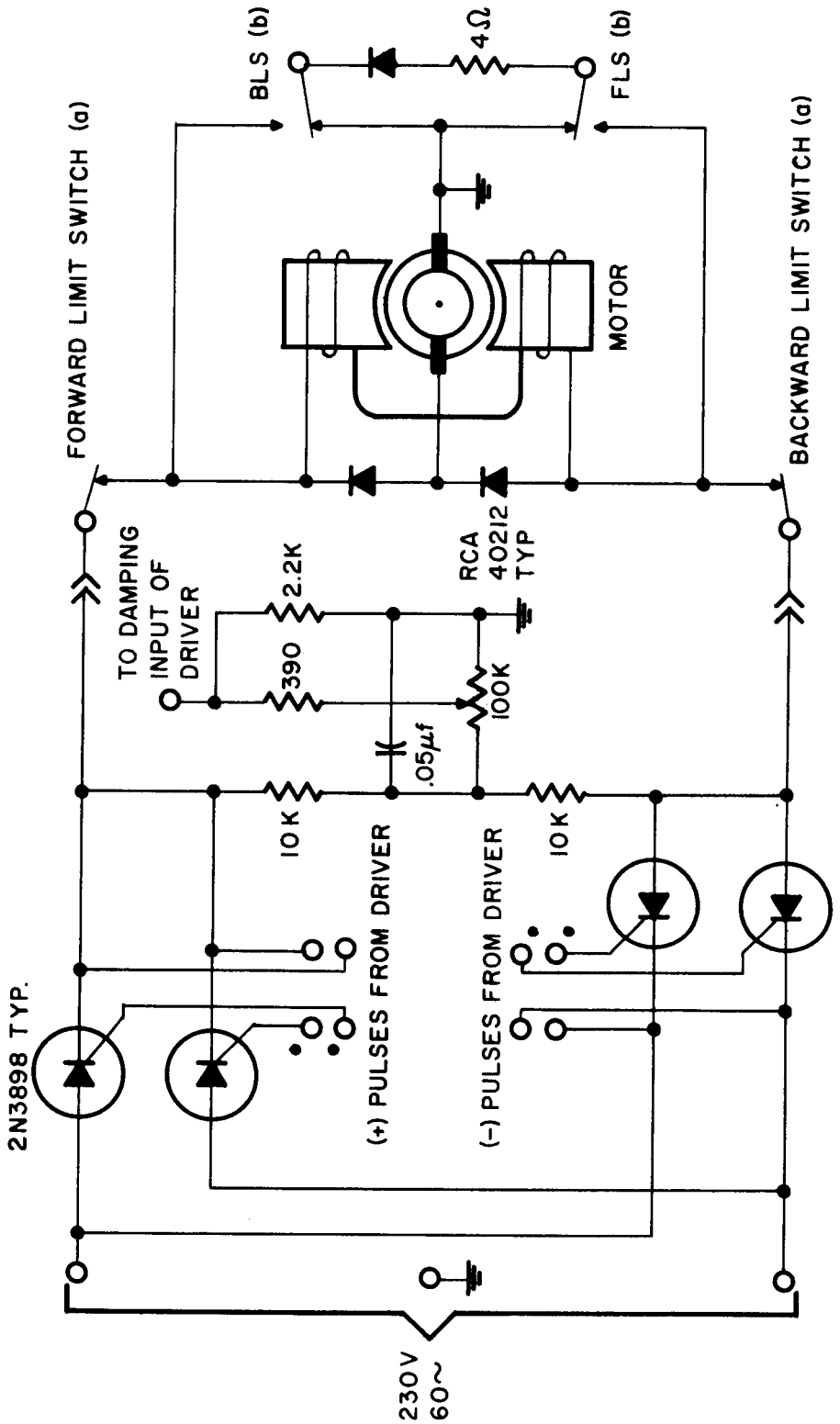

FIGURE 24: OUTPUT STAGE SCHEMATIC

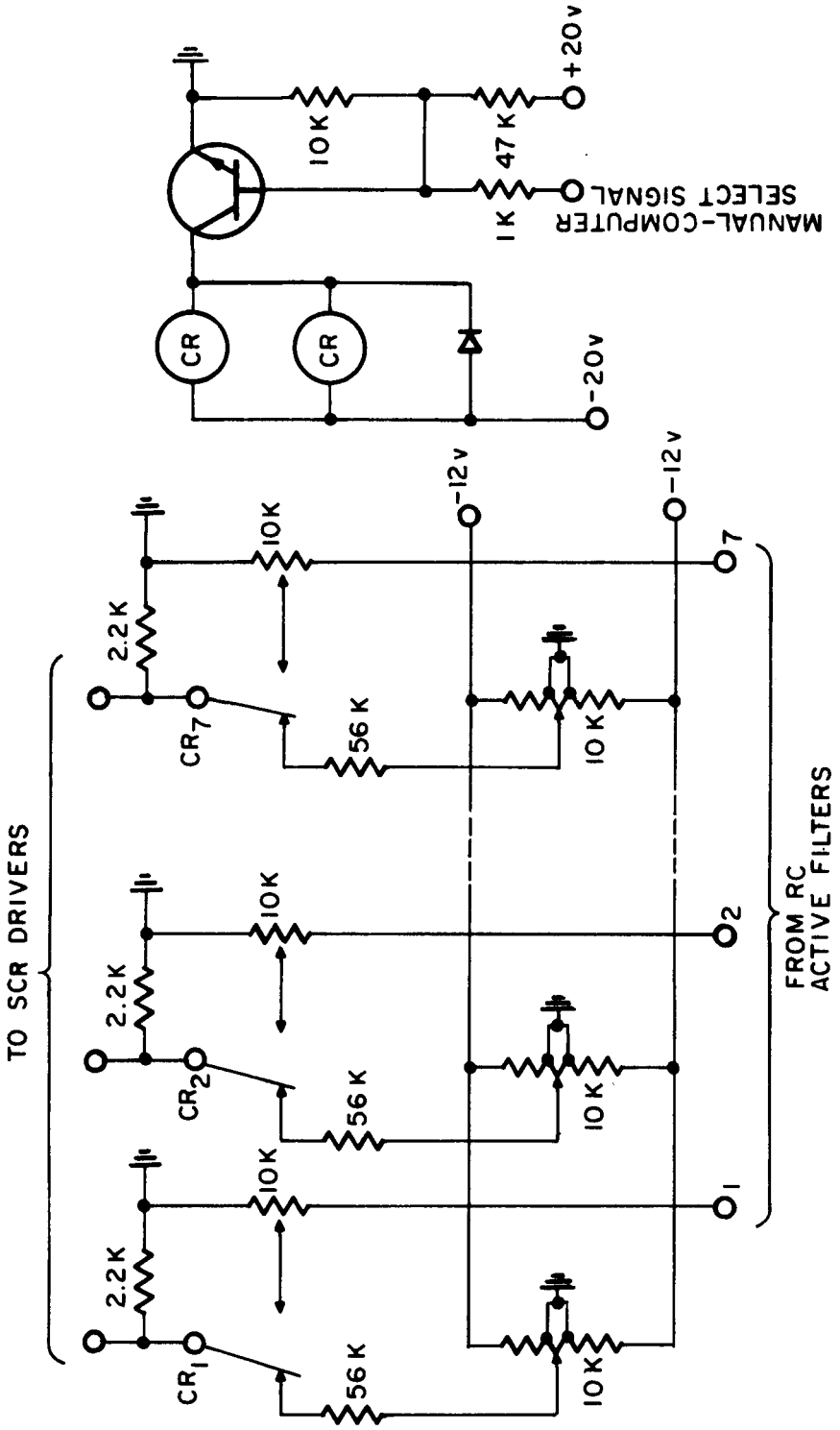

FIGURE 25: MANUAL CONTROL AND SWITCHING RELAY

switching the pulse generators have a grounded input. The manual control voltages are generated by potentiometers which are spring-loaded to return to their center position. Grounded taps in these potentiometers insure that no voltage will be produced in this center position. The automatic control voltages are provided by the RC Active filters, and the gain in this mode can be varied with the 10, 000 ohm potentiometers.

CHAPTER V

DESCRIPTION OF HARDWARE

Packaging

With the exception of the manual controller, the digital-to-analog convertors, and the motors and potentiometers on the manipulator; the entire data conversion system is housed in three and one-half cubic feet of cabinet space. The package is shown in Figure 26. Vertical heat-sinks in back mount the SCR's, and are hinged for access. The power supplies and other shared subsystems are mounted in the lower half of the chassis; the pulse generators and filters are on cards plugged into the top. All connections are made along the side in back; all controls and adjustments are on the front panel.

The manual control panel is shown in Figure 27. It is normally placed in the computer room. In addition to seven proportional-control levers, it includes a power-on switch, a computer over-ride switch, and two-speed control levers for closing and rotating the hand.

The digital-to-analog converters are built on five by seven inch cards and mounted in card cages with the data handling logic. Figure 28 shows one of these cards. Figure 29 shows the R.C.

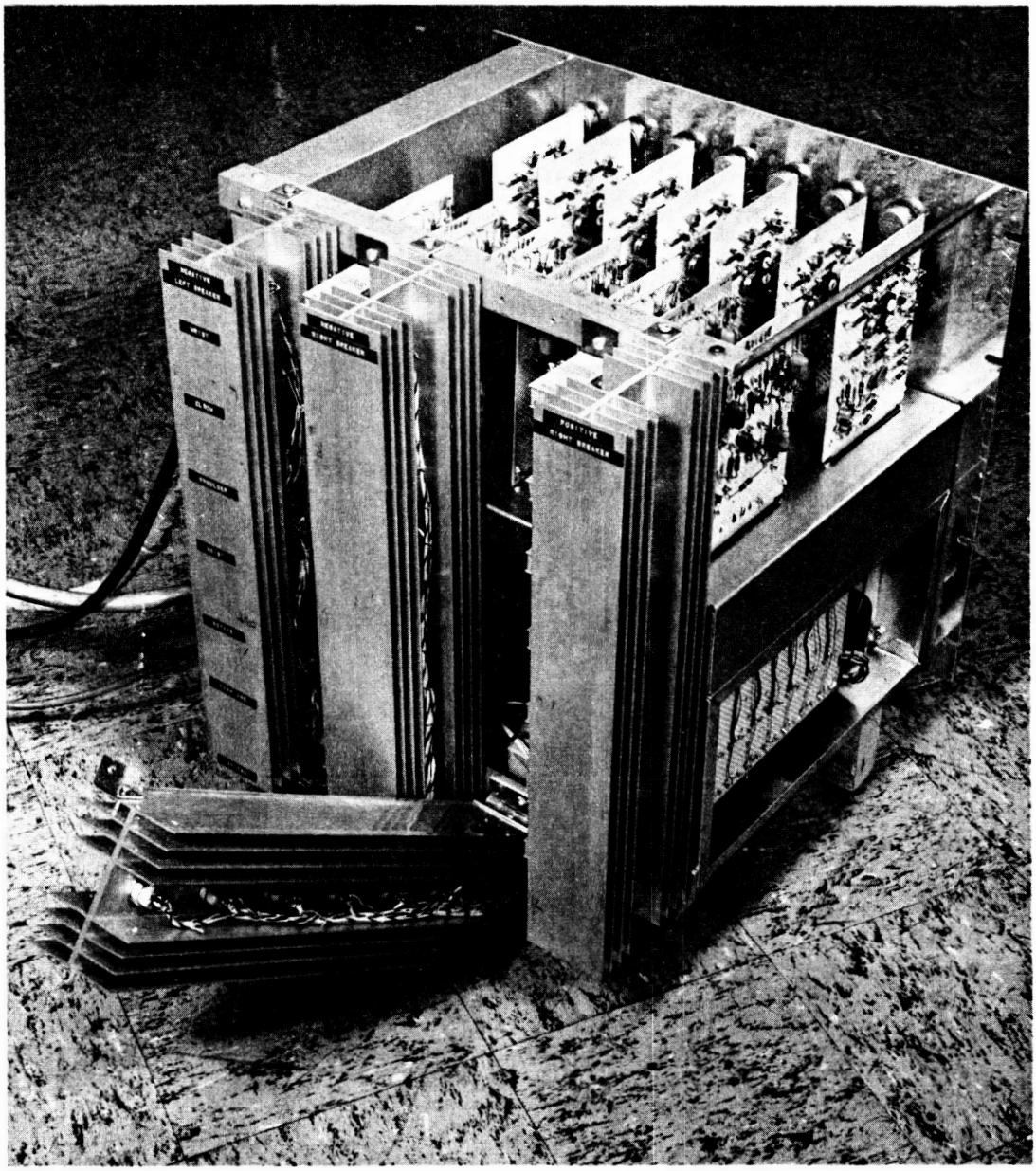

FIGURE 26: MAIN DATA CONVERSION CHASSIS

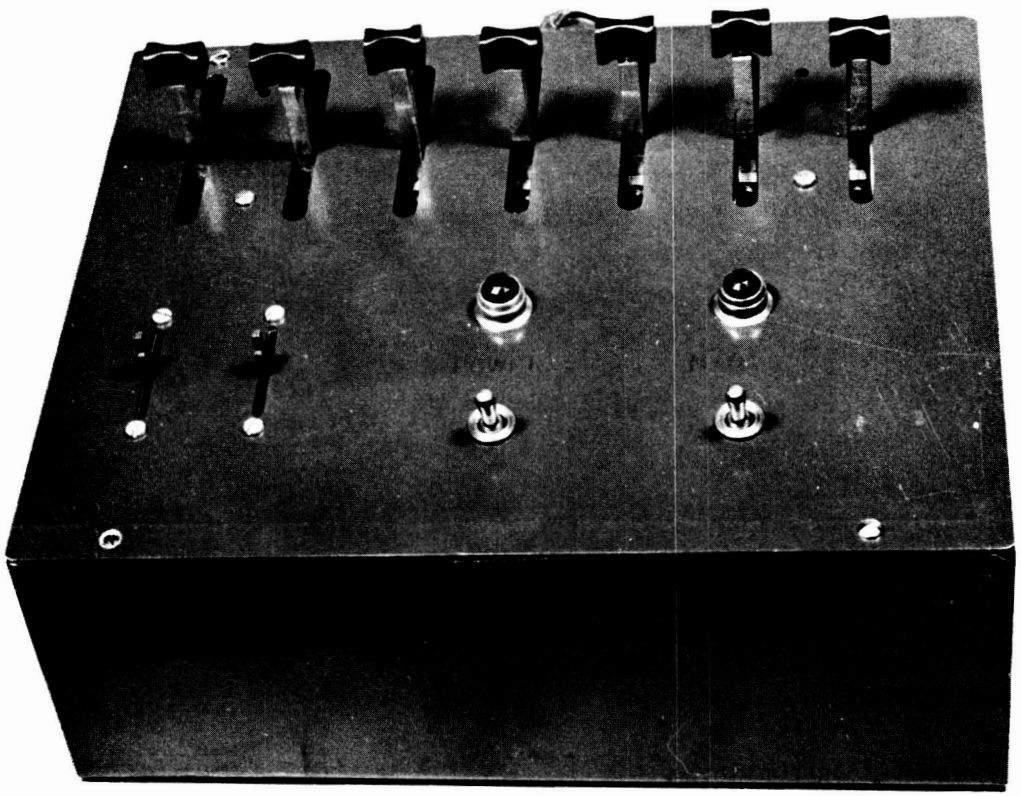

FIGURE 27: MANUAL CONTROL PANEL

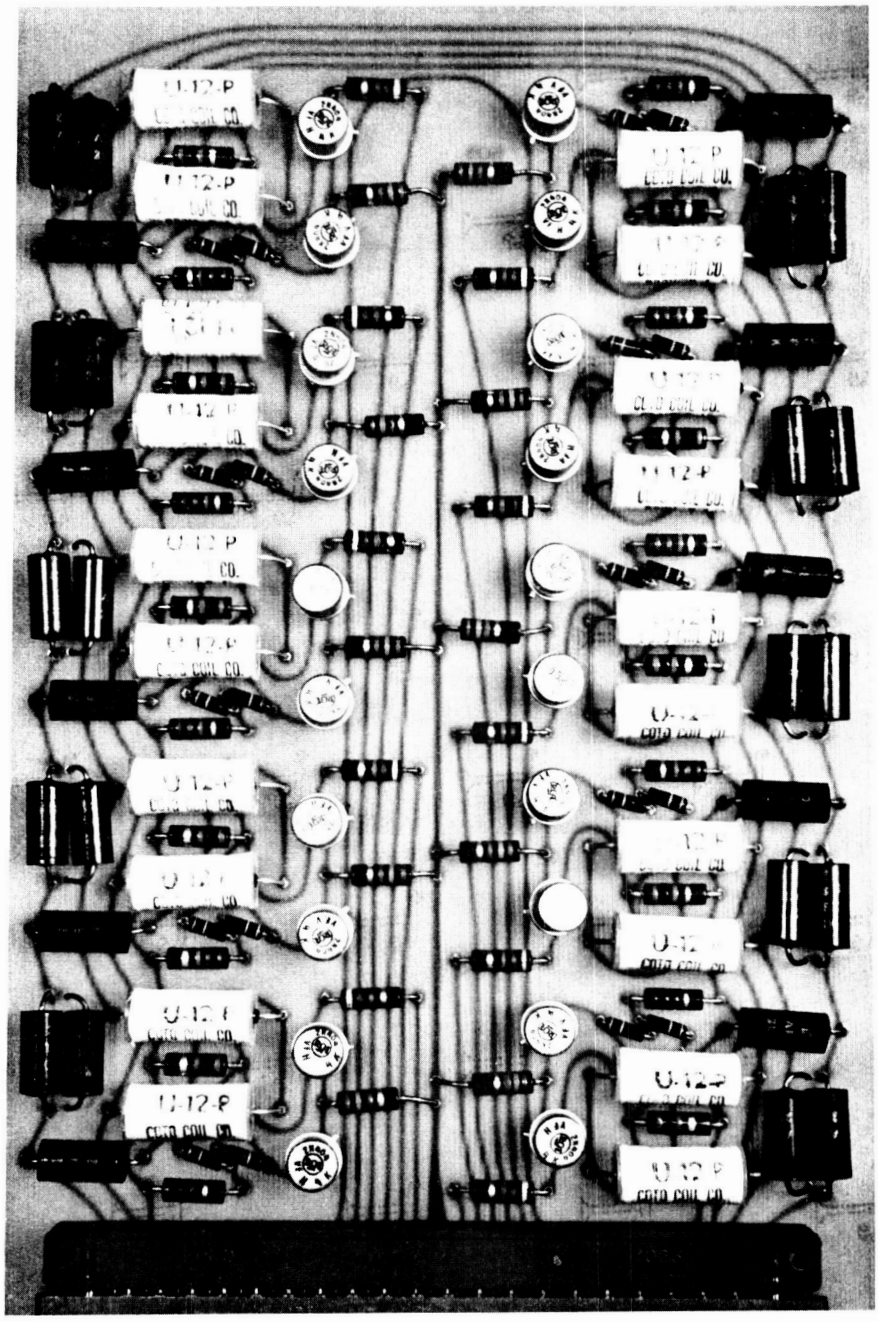

FIGURE 28: DIGITAL TO ANALOG CONVERTOR CARD

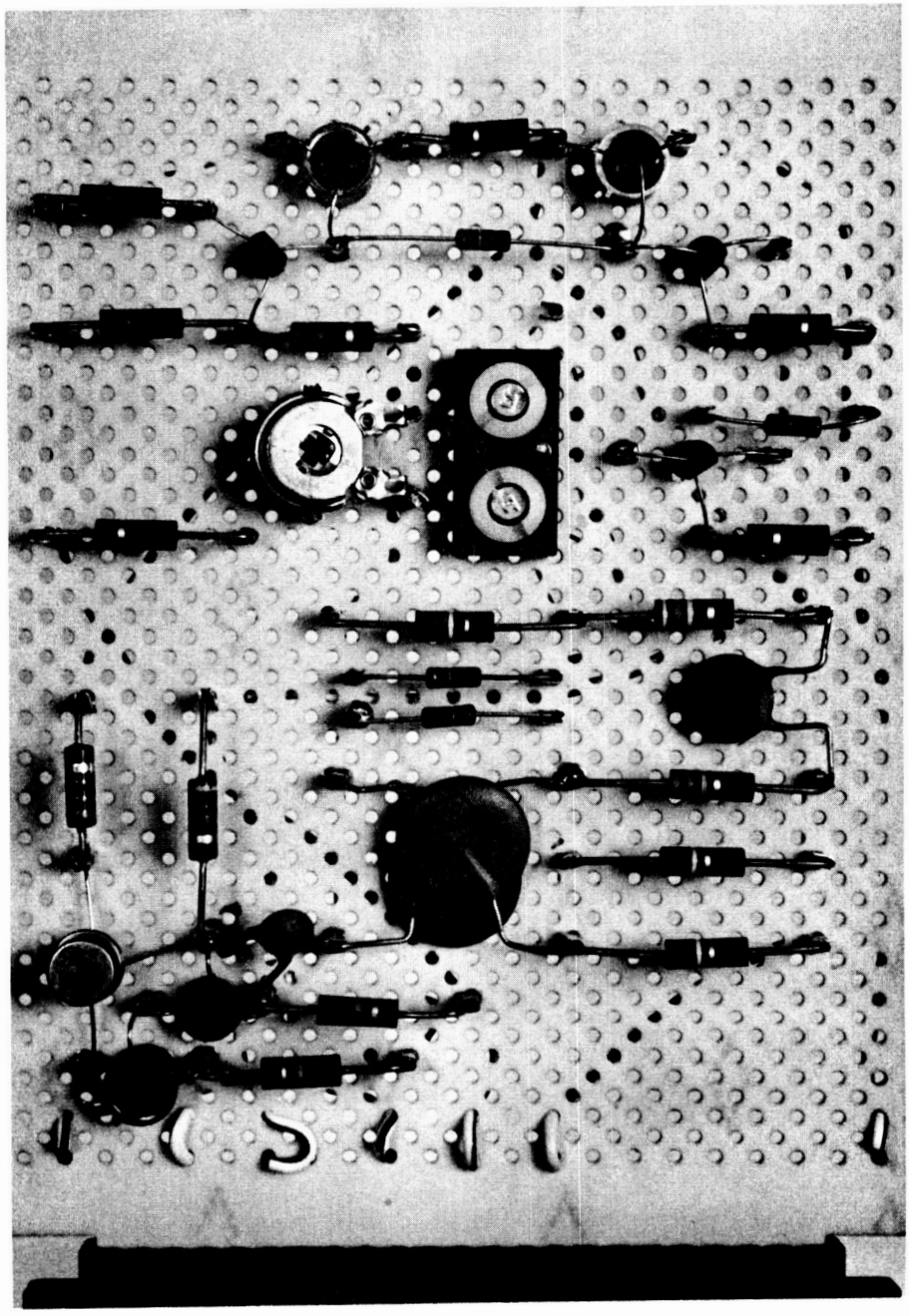

Figure 29: FILTER AND NULL DETECTOR CARD

Active Filter and Null Detector card. Figure 30 shows the SCR pulse generator.

Response

Figure 31 shows the error signal during the reaction of one channel to a step input. The upper trace represents the bridge output, and the lower trace the filter output. The step corresponded to 128 bits, or one-eighth the total travel. The time required for this distance was 5.2 seconds, during virtually all of which the SCR drive was saturated. There is very little over-shoot ringing, and the noise present on the bridge output is effectively removed by the filter.

Cost

The material costs for the data conversion section including motors and potentiometers are approximately $200 per channel.

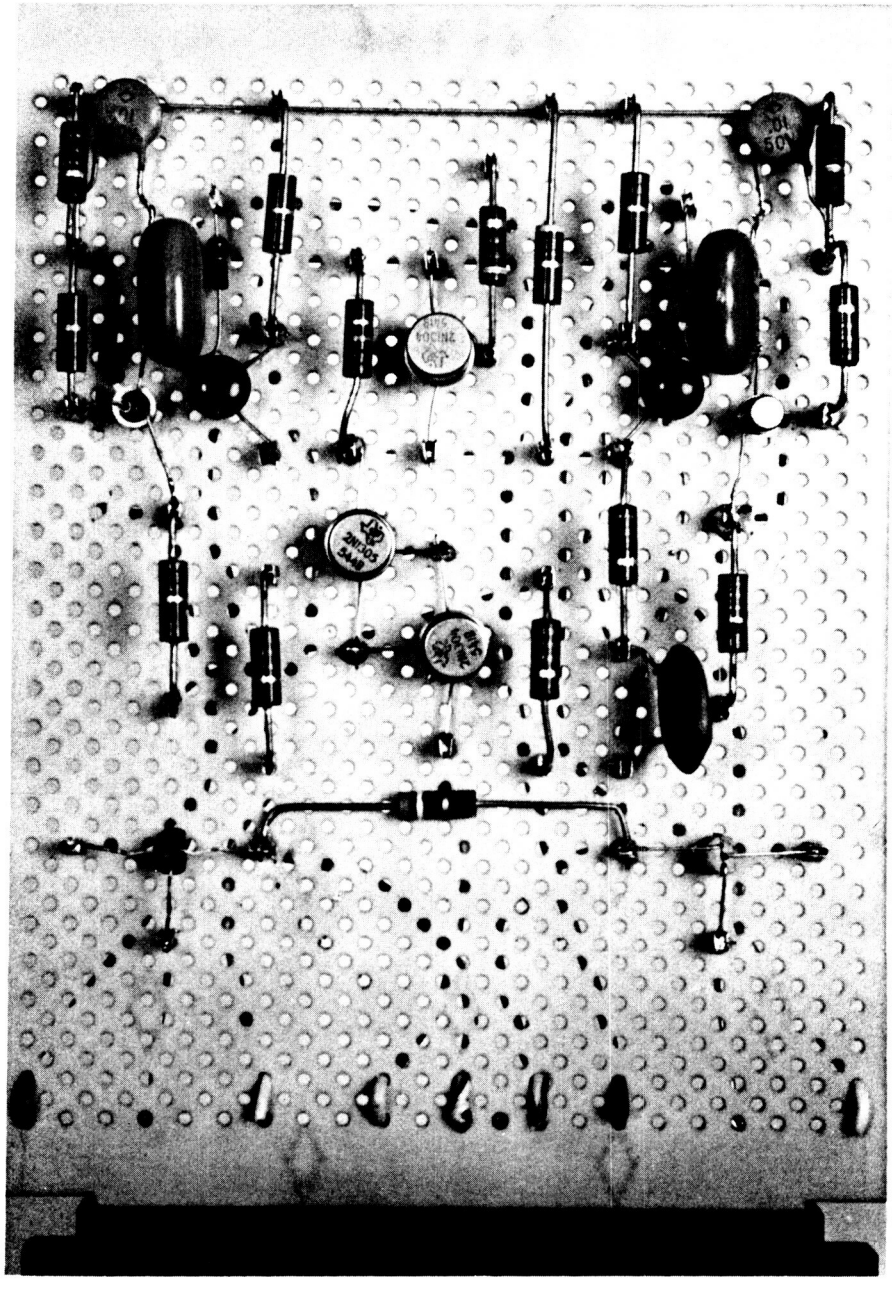

FIGURE 30: PULSE GENERATOR CARD

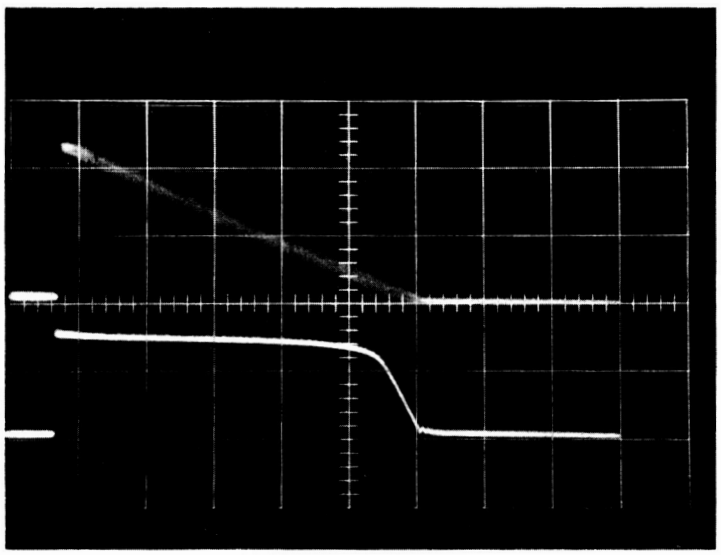

Vertical scale :

2 volts per division

Horizontal scale :

1 second per division

FIGURE 31: SYSTEM STEP RESPONSE

APPENDIX A

A SIMPLE MANIPULATOR CONTROL PROGRAM

Objective

Early in the manipulating studies at Case, a simple program was developed to illustrate computer assisted control of a remote manipulator. This program was based on the assumption that the operator would somehow specify the desired location and orientation of the manipulator hand, and that the computer would generate the motions required to attain them. No concern was given to ensuring that only legal configurations were assumed.

Redundancies

Only five variables are necessary to define the desired hand location and orientation. However, it was assumed that the manipulator had seven degrees-of-freedom. Thus two redundancies exist. For simplicity, the hand co-ordinates were constrained to move linearly with time, and the redundancies were to assume optimum valves on the basis of the program criterion.

Optimization Scheme

The program criterion chosen for optimizing is the minimization of the sum of the momenta of the seven degrees-of freedom. As the hand moves toward its objective, the redundant variables adopt successive values that minimize the total instantaneous momentum. Because of its point-by-point approach this criterion does not optimize the total path of the manipulator, but it does provide an insight into the problems involved.

Manipulator Model

The seven degrees-of-freedom of the manipulator were estimated to have the following masses or inertias:

Degree-of-Freedom	Inertia
X-axis (Bridge)	51 slugs
Y-axis (Carriage)	40 slugs
Z-axis (Hoist)	21 slugs
S-pivot (Shoulder)	7.6 slug-ft^2
E-pivot (Elbow)	4.6 slug-ft^2
W-pivot (Wrist)	2.0 slug-ft^2
θ-pivot (Shoulder rotation)	$6.2\sin^2(S) + 4.2\sin^2(E) + 8.4\sin(S)\sin(E)$ slug-ft^2

(1)

For the interpretation of the nomenclature see Figure 2. The inertia of the shoulder rotation depends on the configuration of the arm of the manipulator.

Analysis

The criterion function, that is the sum of the momenta of the degrees of freedom, on an incremental basis is:

$$F = |I_W SW| + |I_E DE| + |I_S DS| + |I_\theta D\theta| + |I_X DX| + |I_Y DY| + |I_Z DZ| \quad (2)$$

Where D implies a small increment occuring during a time interval Dt. I_W is the wrist inertia, etc.

The co-ordinates of the hand are related to the manipulator variables as follows:

(hand aximuth) = θ

e (hand elevation) = W

x (hand ordinate) =

$$X + \cos(\theta)\ 1.5\sin(S) + 1.5\sin(E) + 1.7\sin(W)$$

y (hand absicca) = (3)

$$Y + \sin(\theta)\ 1.5\sin(S) + 1.5\ \sin(E) + 1.7\sin(W)|$$

z (hand height) =

$$Z + 1.5\cos(S) + 1.5\cos(E) + 1.7\ \cos(W)$$

If the shoulder and elbow are arbitrarily chosen as

the redundant variables, we can write:

$$\theta = a$$

$$W = e$$

$$X = x - \cos(a)\,\left|1.5\sin(S) + 1.5\sin(E) + 1.7\sin(e)\right|$$

$$Y = y - \sin(a)\,\left|1.5\sin(S) + 1.5\sin(E) + 1.7\sin(e)\right| \qquad (4)$$

$$Z = z - 1.5\cos(S) - 1.5\cos(E) - 1.7\cos(e)$$

For small increments, these become:

$$D\theta = Da$$

$$DW = De \qquad (5)$$

$$DX = Dx - Da\sin(a)\,\left|1.5\sin(S) + 1.5\sin(E) + 1.7\sin(e)\right|$$

$$- \cos(a)\left|1.5DS\cos(S) + 1.5DE\cos(E) + 1.7De\cos(e)\right|$$

$$DY = Dy + Da\cos(a)\,\left|1.5DS\sin(S) + 1.5\sin(E) + 1.7D\cos(e)\right|$$

$$- \sin(a)\,\left|1.5DS\cos(S) + 1.5DE\cos(E) + 1.7\,e\cos(e)\right|$$

$$DZ = Dz + 1.5DS\sin(S) + 1.5DE\sin(E) + 1.7De\sin(e)$$

When these expressions are substituted into the criterion function, it can be evaluated in terms of the hand co-ordinates and the two redundancies. If all parameters except DE and DS are held fixed, the criterion function takes the form:

$$F = \sum_{i=1}^{6} (a_i DE + b_i DS + c_i) + k \qquad (6)$$

Each of the terms of the summation is a linear equation

in two variables, and the plot of its magnitude is a plane surface reflecting off the DE, DS plane at the line $a_i DE + b_i DS + c_i = 0$. The sum of such surfaces is also planar except over the six reflection lines, where there are ridges. It is easy to show that the minimum value of such a surface lies above one of the intersections of these reflection lines.

The minimum can only lie on one of the planar facets if that facet is level; in which case we may arbitrarily locate it at the edge, i.e., on a ridge.

The minimum can only lie on one of the ridges if that ridge is horizontal; in which case we may arbitrarily locate it at one end of the ridge, i.i., at a ridge intersection.

Hence the minimum can always be found at a ridge intersection, or directly over a reflection line intersection. But six coplanar lines can intersect in at most $1/2\ (6)\ (6-1) = 15$ points. Thus rather than employing a statistical two variable search to find the minimum of F, we need only find the 15 intersections of the reflection lines, evaluate F at each point, and choose the smallest value. This is an advantage of this choice of criterion function.

The manipulator path is generated in the following iterative manner: the computer has available from the interface the initial values of the manipulator variables. From the desired hand co-ordinates given by the operator, it computes the number and size of the increments necessary. It then advances through the following steps:

1. All the coefficients a_i, b_i, and c_i are evaluated in equation (6).

2. The intersection of a pair of reflection lines $a_i DE + b_i DS + c_i = 0$ and $a_j DE + b_j DS + c_j = 0$ is found through simultaneous solution, that is:

$$DE = \frac{c_j b_i - c_i b_j}{a_i b_j - a_j b_i} \qquad DS = \frac{c_i a_j - c_j a_i}{a_i b_j - a_j b_i} \qquad (7)$$

3. The criterion function is evaluated at this intersection point, using the coefficients calculated in step 1.

4. A running variable, F_{min}, is compared with this new value of F; and if F is smaller, then F_{min} assumes the value of F. F_{min} is initially defined to be very large to insure that it assumes the first value calculated. On completion of this step the computer returns to step 2. Thus after all 15 values have been observed F_{min} will take on the smallest of them. Similar running variables identify the values of

DE and DS that gave the best criterion.

5. The best values of DE and DS are added on to the previous values to obtain the "initial conditions" for the next step. The increments Dx, Dy, Dz, Dϕ, Dc are also added to their previous values. The new manipulator variables are computed from equations (4). Using these new values, the computer returns to step 1 and begins again.

6. A running variable counts up the number of times the above loop has been executed, and stops the process after a specified number has been reached.

This algorithm is illustrated in the flow chart of Figure 32. An Algol realization of this program was written for the Univac 1107. Several different simulations on this computer revealed the deficiencies of a point-by-point optimization scheme for long translations, although it performs as designed. For practical manipulator control a considerably more sophisticated program is required[3], but the basic principles are similar.

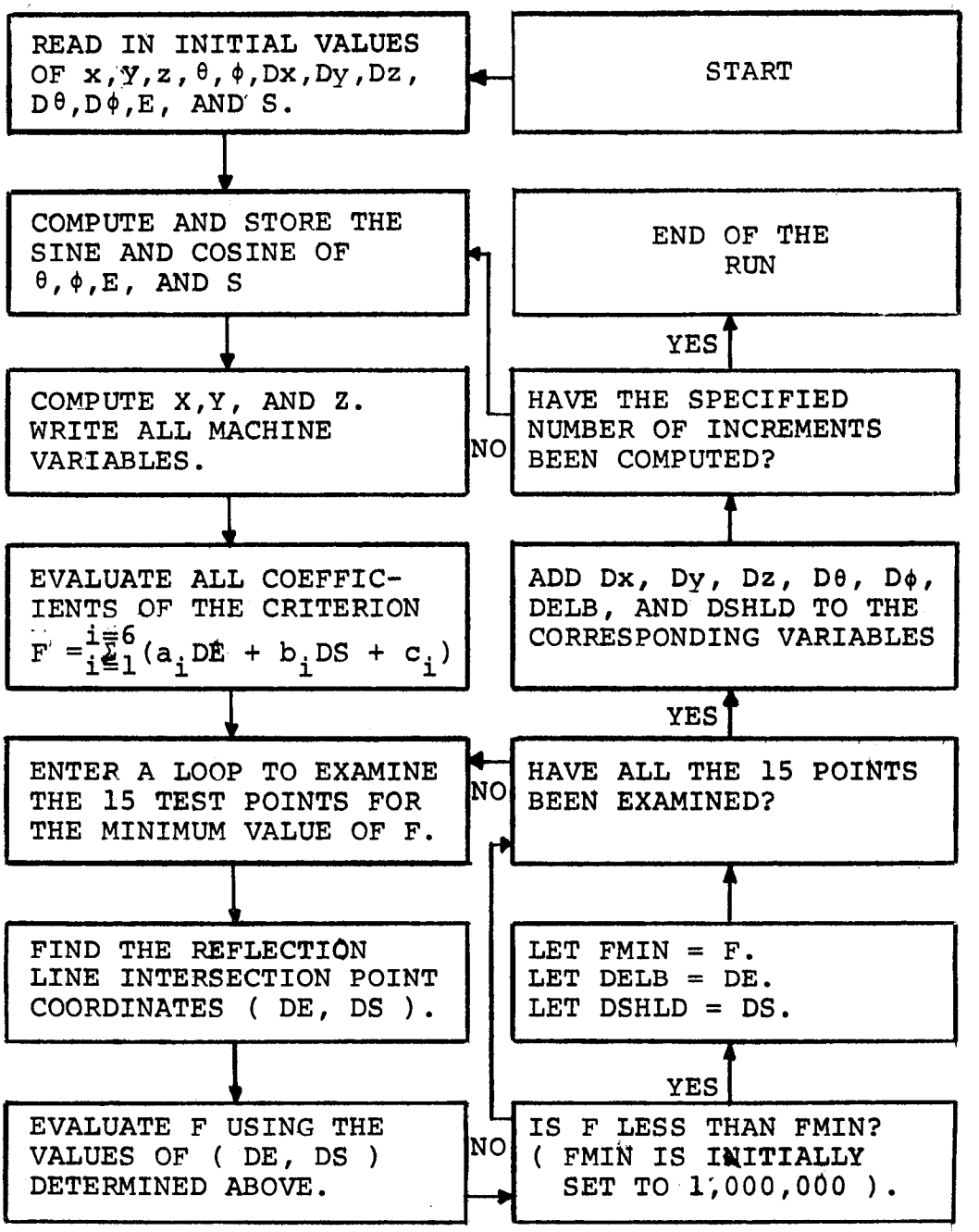

FIGURE 32: ALGORITHM FLOW CHART

BIBLIOGRAPHY

1. Johnsen, E.G., "Proceedings of the 1964 Seminars on Remotely Operated Special Equipment", Volumes I and II, USAEC reports CONF640508 and CONF641120

2. Taylor, R.J., M.S. Thesis (pending), Case Institute of Technology.

3. Beckett, J.T., Ph.D. Thesis (pending), Case Institute of Technology.

4. Mergler, H. W., et.al., "Digital Control Systems Engineering", Case Institute of Technology Summer Program Notes, 1962

5. Joseph, R. D., "R.C. Active Network Design Using Unity Gain Amplifiers", IEEE Circuit Theory Presentation, Cleveland Section, March 15, 1965.

6. Balabanian, N., "Active R.C. Network Synthesis," Armed Services Technical Information Agency Number AD 270613, December, 1961.

7. Sevin, L.J., "Field Effect Transistors," McGraw-Hill Book Company, 1965.

8. Truxal, J. G., "Control Engineers' Handbook", McGraw-Hill Book Company, 1958.